CONTRIBUTION FROM THE DEPARTMENT OF CHEMISTRY,
COLUMBIA UNIVERSITY, NEW YORK, NEW YORK 10027

Electronic Structures of Metal Pentacyanonitrosyls

BY P. T. MANOHARAN AND HARRY B. GRAY[1]

Received December 15, 1965

The bonding in transition metal pentacyanonitrosyls is described in terms of molecular orbitals. The very strong M–NO bond dominates the over-all ligand field, where M is the transition metal. Detailed SCCC–MO calculations of $M(CN)_5NO^{n-}$ complexes give the d-level ordering $xz,yz < xy < x^2 - y^2 < z^2$, suggesting some axial destabilization of z^2. The most important result is that the antibonding e level derived from π^*NO is the lowest empty level in the $M(CN)_5NO^{n-}$ complexes. The electronic absorption bands of the $M(CN)_5NO^{n-}$ complexes are assigned using the derived energy level scheme. In certain cases substantial support comes from single crystal spectra using polarized light and the glass spectra of $[(n\text{-}C_4H_9)_4N]_m[M(CN)_5NO]$ complexes at liquid-nitrogen temperature. The most important new result is the assignment of the low-energy bands as due to charge-transfer transitions from the metal-based e and b_2 levels to the unusually stable $e(\pi^*NO)$ level. The derived molecular orbitals have been used to calculate the spin Hamiltonian parameters of the paramagnetic species $Mn(CN)_5NO^{2-}$ and $Cr(CN)_5NO^{3-}$. Agreement between the calculated and measured spin Hamiltonian parameters indicates the reliability of the derived molecular orbitals.

Introduction

The electronic structure of $Fe(CN)_5NO^{2-}$ has been established on the basis of considerable experimental and theoretical work.[2] In the attempts[3-10] in the area of assignments of the low-energy electronic absorption bands in the other $M(CN)_5NO^{n-}$ complexes, no consideration has been given to the π^*NO level, which plays an important role in the low-energy bands in $Fe(CN)_5NO^{2-}$. It is clear that the possibility of low-energy charge-transfer bands in all these complexes must be considered.

This paper reports detailed SCCC–MO (self-consistent charge and configuration–molecular orbital) calculations of the complexes $M(CN)_5NO^{n-}$ (M = V, Cr, Mn, Fe), electronic absorption spectra of $M(CN)_5NO^{n-}$ complexes in solutions at room temperature and at low temperature, additional single crystal spectra of $Na_2Fe(CN)_5NO\cdot 2H_2O$ using polarized light, and an esr study[11] of $K_2Mn(CN)_5NO$ in a single crystal of $Na_2Fe(CN)_5NO\cdot 2H_2O$ as host lattice. The electronic spectral and esr results are interpreted in terms of the derived molecular orbitals for the $M(CN)_5NO^{n-}$ complexes.

Experimental Section

Preparation of Various $M(CN)_5NO^{n-}$ Complexes.—Reagent grade $Na_2Fe(CN)_5NO\cdot 2H_2O$ was crystallized from water solution before use. The other pentacyanonitrosyls, $K_5V(CN)_5NO\cdot H_2O$,[12a] $K_3Cr(CN)_5NO\cdot H_2O$,[12b] $K_3Mn(CN)_5NO\cdot H_2O$,[13] and $K_2Mn(CN)_5NO$,[13] were prepared and purified by literature methods. The paramagnetic manganese compound, $K_2Mn(CN)_5NO$, was stored over P_2O_5 in a desiccator. The sodium salt of $Mn(CN)_5NO^{2-}$ also was prepared. All the compounds were stored in air-tight containers.

Preparation of *n*-Tetrabutylammonium Salts of the $M(CN)_5NO^{n-}$ Complex Anions.—The $[(n\text{-}C_4H_9)_4N)]_m[M(CN)_5NO]$ complexes were needed for the spectral measurements in transparent glasses at low temperatures and also for infrared spectral measurements. The $[(n\text{-}C_4H_9)_4N]_2[Fe(CN)_5NO]$ complex was prepared by thoroughly mixing a 0.03 *M* aqueous solution of $Na_2Fe(CN)_5NO\cdot 2H_2O$ with a 0.03 *M* chloroform solution of $[(n\text{-}C_4H_9)_4N]Br$. The chloroform layer was separated and the solvent was stripped. The residue was then repeatedly extracted with water-free chloroform and the solvent was completely removed. The resulting red compound was dried over anhydrous $CaCl_2$ in a desiccator.

The *n*-tetrabutylammonium salts of $Mn(CN)_5NO^{3-}$ and $Cr(CN)_5NO^{3-}$ were prepared in the above manner. The former complex was obtained as a violet powder and the latter one as a greenish yellow crystalline compound. A small quantity of *n*-tetrabutylammonium bromide remained in all these compounds and could not be removed completely.

In the preparation of $[(n\text{-}C_4H_9)_4N]_2[Mn(CN)_5NO]$, equivalent quantities of $K_2Mn(CN)_5NO$, dried over P_2O_5 in a desiccator, and $[(n\text{-}C_4H_9)_4N]Cl$, dried over anhydrous $CaCl_2$ in a desiccator, were dissolved in very dry acetone. The precipitated KCl and other impurities were removed by rapid filtration and the solvent was stripped. The residue was then dissolved in half the volume of acetone than was previously used; the solution was filtered and the solvent was stripped. This was repeated three times to purify the *n*-tetrabutylammonium salt. The yellow compound was then dried over P_2O_5 in a desiccator. The acetone used in this preparation had been dried over anhydrous $MgSO_4$ and anhydrous K_2CO_3 and then distilled. The middle fraction was used. This precaution was necessary since the presence of water in small amounts slowly decomposes $K_2Mn(CN)_5NO$.

EPA Solvent for Low-Temperature Absorption Spectra.—EPA solvent, a mixture of ethyl alcohol, isopentane, and ethyl ether in 2:5:5 volume proportion, was obtained from Hartmann-Leddon Co. It forms a perfect glass at liquid nitrogen temperature and is optically transparent in the region 1000–270 mμ. Since even minute quantities of water in the solvent tend to crack the glass, great care was taken to keep it dry. EPA was used as a glassy matrix for the low-temperature spectra of the various $M(CN)_5NO^{n-}$ complexes.

(1) Alfred P. Sloan Research Fellow.

(2) (a) P. T. Manoharan and H. B. Gray, *J. Am. Chem. Soc.*, **87**, 3340 (1965).

(3) H. B. Gray, P. T. Manoharan, J. Pearlman, and R. F. Riley, *Chem. Commun.* (London), 62 (1965).

(4) I. Bernal and S. E. Harrison, *J. Chem. Phys.*, **34**, 102 (1961).

(5) C. S. Naiman, *ibid.*, **35**, 1503 (1961).

(6) H. B. Gray and C. J. Ballhausen, *ibid.*, **36**, 1151 (1962).

(7) Y. J. Israeli, *Bull. Soc. Chim. France*, 1145 (1964).

(8) H. A. Kuska and M. T. Rogers, *J. Chem. Phys.*, **42**, 3034 (1965).

(9) (a) J. Danon, *ibid.*, **41**, 3378 (1964); (b) J. Danon, R. P. A. Nuniz, and H. Panapucci, *ibid.*, **41**, 3651 (1964).

(10) B. Jezowska-Trzebiakowska, "Theory and Structure of Complex Compounds," The Macmillan Co., New York, N. Y., 1964.

(11) A preliminary report of this work has been published: P. T. Manoharan and H. B. Gray, *Chem. Commun.* (London), 324 (1965).

(12) (a) W. P. Griffith, J. Lewis, and G. Wilkinson, *J. Chem. Soc.*, 1632 (1959); (b) *ibid.*, 872 (1959).

(13) F. A. Cotton, R. R. Monchamp, R. J. M. Henry, and R. C. Young, *J. Inorg. Nucl. Chem.*, **10**, 28 (1959).

$Na_2Fe(CN)_5NO\cdot 2H_2O$ for Single Crystal Spectra.—For the single crystal absorption spectra of $Na_2Fe(CN)_5NO\cdot 2H_2O$, crystals of a few microns in thickness were used. A very dilute solution of recrystallized sodium nitroprusside in water was evaporated rapidly by pouring on a flat dish. The crystals formed and were collected and dried with a filter paper. The faces could be easily identified under a microscope.

Dilute Single Crystals for Esr Experiments on $Mn(CN)_5NO^{2-}$.—A 1.5-g quantity of recrystallized sodium nitroprusside and 0.005 g of $K_2Mn(CN)_5NO$ were dissolved in 30 ml of water. The solution was filtered by using a sinter to remove all insoluble impurities. The filtrate was placed in a dark cupboard and, after a few days of evaporation, crystals of sufficient thickness were formed. They were removed before the solvent completely evaporated and washed with a very minute quantity of water over a filter to remove any adhering particles on the various faces. The crystals had very well-developed faces. In some experiments, $Na_2Mn(CN)_5NO$ was used instead of $K_2Mn(CN)_5NO$.

Physical Measurements. Solution Spectra.—Aqueous solution electronic spectra of all the $M(CN)_5NO^{n-}$ complexes were obtained using a Cary Model 14 spectrophotometer. No difficulty was encountered in the measurements except in the case of $K_2Mn(CN)_5NO$. In the measurement of electronic spectra of $K_2Mn(CN)_5NO$, aqueous solutions were satisfactory in the region 600–190 mμ. However, the solution had to be prepared freshly before each measurement, since aqueous solutions of $K_2Mn(CN)_5NO$ decompose slowly, as judged by the precipitation of oxides of manganese. Spectral measurements in the near-infrared region were more difficult because aqueous solutions gave an instantaneous precipitate in the presence of near-infrared radiation. The resulting solution was violet, indicating the presence of $Mn(CN)_5NO^{3-}$. This difficulty in measuring the spectrum of $K_2Mn(CN)_5NO$ in the near-infrared region was overcome by using spectral grade acetonitrile as solvent and well-dried $K_2Mn(CN)_5NO$. In this medium the $Mn(CN)_5NO^{2-}$ complex is not immediately reduced on absorbing near-infrared radiation.

Low-Temperature Spectra.—Low-temperature absorption spectra were measured in an EPA glass containing $[(n\text{-}C_4H_9)_4N]_m[M(CN)_5NO]$. The spectra were obtained with a Cary Model 14 spectrophotometer, using a cold cell fitted inside a quartz dewar with optical windows. Liquid nitrogen was used as a coolant and the temperature was measured with an iron–constantan thermocouple. The measured low-temperature spectra were corrected for solvent contraction, using the data of Passerani and Ross.[14]

Infrared Spectra.—Infrared spectra of some of the $[(n\text{-}C_4H_9)_4N]_m[M(CN)_5NO]$ compounds were measured with chloroform as solvent using a Perkin-Elmer 421 grating spectrophotometer. The spectra of KBr pellets were also measured in the region 1000–250 cm^{-1} for some of the potassium and sodium salts of the pentacyanonitrosyls, using a Perkin-Elmer 521 grating spectrophotometer.

Magnetic Susceptibility Measurements.—Static susceptibility measurements of solid $K_2Mn(CN)_5NO$ were made at room temperature by the Gouy method using $Hg[Co(SCN)_4]$ as calibrant.[15]

Single Crystal Absorption Spectra of $Na_2Fe(CN)_5NO\cdot 2H_2O$.—Single crystal absorption spectra were obtained with a microspectrophotometer based on a modified Leitz polarizing microscope, designed at the Yale University Chemistry Department. The light was rendered plane polarized by a Glan prism, the polarization of the incident beam was fixed, and the crystal was rotated on a mount. The procedure used to obtain both the uncorrected and corrected spectra has been given.[2]

Results

Single Crystal Esr Spectra of $Mn(CN)_5NO^{2-}$ in a Host Lattice of $Na_2Fe(CN)_5NO\cdot 2H_2O$.—For Mn^{2+} in $Mn(CN)_5NO^{2-}$, which has axial symmetry, the spin Hamiltonian is[16]

$$\mathcal{H} = \beta[g_{\parallel}H_zS_z + g_{\perp}(H_xS_x + H_yS_y)] + AS_zI_z + B(S_xI_x + S_yI_y) \quad (1)$$

where $\parallel$ and $\perp$ refer to the directions parallel and perpendicular to the symmetry axis NC–Fe–NO. To include the nitrogen extrahyperfine structure, the Hamiltonian is given by

$$\mathcal{H} = \beta[g_{\parallel}H_zS_z + g_{\perp}(H_xS_x + H_yS_y)] + A^{Mn}S_zI_z^{Mn} + B^{Mn}(S_xI_x^{Mn} + S_yI_y^{Mn}) + A^{N}S_zI_z^{N} + B^{N}(S_xI_x^{N} + S_yI_y^{N}) \quad (2)$$

where S, I^{Mn}, and I^{N} refer to the electron spin and manganese and nitrogen nuclear spins, respectively. A and B are the hyperfine splittings when the applied field H is parallel and perpendicular, respectively, to the symmetry axis. β is the Bohr Magneton.

Considering the second-order interaction with the manganese nuclear spin alone, neglecting quadrupole interaction, the transition energies allowed by the selection rules $\Delta M = \pm 1$, $\Delta m = 0$ are given by the relation

$$h\nu = g\beta H + Km + \frac{B^2}{4g\beta H_0}\frac{[A^2 + K^2)}{K^2}[I(I+1) - m^2] \quad (3)$$

where M is the electron spin quantum number and ν is the microwave frequency. Also

$$g^2K^2 = A^2g_{\parallel}^2\cos^2\theta + B^2g_{\perp}^2\sin^2\theta \quad (4)$$

$$g^2 = g_{\parallel}^2\cos^3\theta + g_{\perp}^2\sin^2\theta \quad (5)$$

where θ is the angle between the symmetry axis and the applied field H. H_0 is defined by $h\nu = g\beta H_0$; that is, in the absence of hyperfine splitting all the lines would coincide and occur at this field. The first-order interaction should produce $2I + 1$ equally-spaced lines whereas the second-order term should later cause deviations from the equal spacings, as observed in the esr spectra of $Mn(CN)_5NO^{2-}$ ion.

The resonance conditions for $\theta = 0°$, $90°$, and other angles are

$$\theta = 0°;\quad H_{\parallel} = \frac{h\nu}{g_{\perp}\beta} - \frac{A}{g_{\parallel}\beta}m - \frac{B^2}{2(g_{\parallel}\beta)^2H_0}[I(I+1) - m^2] \quad (6)$$

$$\theta = 90°;\ H_{\perp} = \frac{h\nu}{g_{\perp}\beta} - \frac{B}{g_{\perp}\beta}m - \frac{A^2 + B^2}{4(g\beta)^2H_0}[I(I+1) - m^2] \quad (7)$$

$$0° < \theta < 90°;\quad H_{\theta} = \frac{h\nu}{g_{\theta}\beta} - \frac{K}{g_{\theta}\beta} - \frac{B^2}{4(g_{\theta}\beta)^2H_0}[I(I+1) - m^2] \quad (8)$$

(14) R. Passerani and I. G. Ross, *J. Sci. Instr.*, **30**, 274 (1953).

(15) B. N. Figgis and J. Lewis, "Modern Coordination Chemistry," Interscience Publishers, Inc., New York, N. Y., 1960, p 406.

(16) B. Bleaney, *Phil. Mag.*, **42**, 441 (1951).

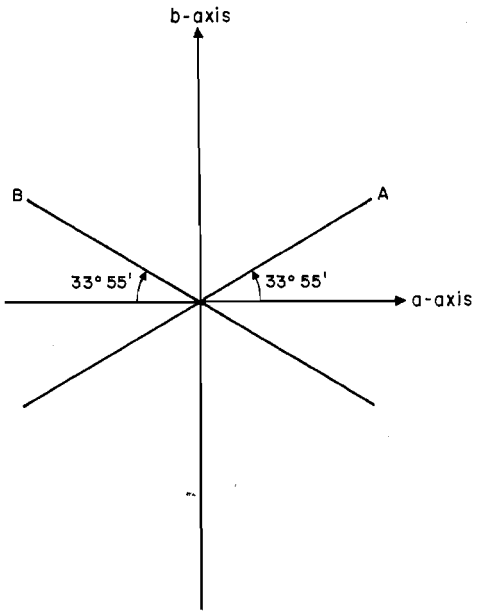

Figure 1.—Orientation of NC–Fe–NO axes in the *ab* plane of the $Na_2Fe(CN)_5NO\cdot 2H_2O$ crystal; the two different orientations are labeled *A* and *B*.

The angular variation of the hyperfine lines can be interpreted with the aid of the above equations.

All esr spectra were obtained at room temperature, using a Varian V-4500 spectrometer employing 100 kc/sec modulation, and the Klystron frequency was directly measured from a wave meter. The field was measured from the previously calibrated field dial. Measurements were made with a crystal of $Na_2Fe(CN)_5NO\cdot 2H_2O$, doped with approximately 0.3% $K_2Mn(CN)_5NO$, of 0.3 × 0.15 × 0.1 cm dimensions. Other crystals, including ones doped with $Na_2Mn(CN)_5NO$ instead of $K_2Mn(CN)_5NO$, gave identical results.

The crystal was mounted with the help of grease on a suitable end of a tiny platform of a polystyrene rod. The polystyrene rod was placed in the microwave cavity. The rod could be rotated and the angle of rotation read to ±0.5°.

The orientation dependence of the spectra was investigated for the *ab* plane, containing the symmetry axes, NC–Mn–NO, in two different orientations *A* and *B*, as shown in Figure 1. The crystal was rotated about the *c* axis, perpendicular to the *ab* plane. The measurements allowed the determination of all the parameters of the spin Hamiltonian given by eq 2. The results are reported in three sections.

(a) First the field H was applied parallel to the crystal *a* axis. Since both orientations *A* and *B* of the symmetry axes are equally inclined at an angle of 33° 55′ to the *a* axis, the six ^{55}Mn hyperfine lines due to both orientations overlap each other and only a six-line spectrum was obtained. In this case, the angle θ, made by the field H with the symmetry axis NC–Mn–NO, is 33° 55′. The triplet separations due to ^{14}N from NO were not well resolved. A very low scan rate gave a partial resolution. The esr spectrum obtained for this orientation is shown in Figure 2a.

(b) The field was applied parallel to the crystal *b* axis, the magnetic plane being the *ab* crystal plane. Here again, both orientations *A* and *B* make the same angle θ = 56° 5′ with the magnetic field H, and a six-line spectrum was obtained due to the overlap of the lines from the two orientations. In this case, however, each of these six lines was resolved further into a triplet, due to the interaction of the electron spin with the $I = 1$ nuclear spin of ^{14}N from the NO. It is reasonable to conclude that these triplets are due to ^{14}N from NO and not from the axial CN because the M–N distance in the axial M–CN is much greater than the one in the M–NO group. This spectrum is shown in Figure 2b.

(c) The crystal was rotated about the crystal *c* axis such that the magnetic field H was not parallel to either the *a* or the *b* axis. Measurements were made at several arbitrary angles. For all the orientations in which the field H is parallel neither to the *a* nor to the *b* axis, the symmetry axes *A* and *B* are differently inclined to the field H. For example, the crystal can be placed in such a way that one of the orientations *A* or *B* is parallel to the field H, *i.e.*, $\theta = 0$. The other orientation, then, makes an angle with the field of θ = 67° 50′. In this experiment a 12-line hyperfine spectrum due to ^{55}Mn was obtained. On the basis of observations from the orientations (a) and (b), the lines with larger separations in which the ^{14}N triplets were not resolved were assigned to $\theta = 0$, and the ones with the smaller separations with well-resolved triplets were assigned to θ = 67° 50′. This spectrum is shown in Figure 2c. Similarly, one of the symmetry axes *A* or *B* was placed perpendicular to the field H (θ = 90°) so that the other orientation made an angle of θ = 22° 10′ with the field H. As before, this gave a 12-line hyperfine spectrum due to the ^{55}Mn nuclear spin, which is shown in Figure 2d. Lines due to θ = 90° were well-resolved triplets. The triplets of the θ = 0° and 22° 10′ orientations were partially resolved for a very low scan rate. Measurements were also made at other angles. Figure 2e shows one of the nitrogen triplets at θ = 67° 50′, when the field H was scanned at a slow rate.

In general, the ^{14}N triplets were fairly well resolved at larger angles. They were analyzed as gaussians and the extrahyperfine constants due to ^{14}N were measured from these triplets. No hyperfine splitting due to the natural abundance ^{13}C from the CN groups was observed. The appearance of forbidden transitions due to $\Delta m = \pm 1$ and $\Delta m = \pm 2$ was observed at the larger θ side of the spectrum. These lines of very low intensities can be seen in the spectrum shown in Figure 2c. The lines were not sufficiently intense to study in detail.

The spin Hamiltonian parameters were obtained from experimental data by solving eq 6, 7, and 8. The relevant parameters for $Mn(CN)_5NO^{2-}$, and for comparison those for $Cr(CN)_5NO^{3-}$, are given in Table I.

Since A^N could not be measured very accurately from the experimental spectrum it was calculated from the equation

$$(A_\theta^N)^2 = (A^N)^2 \cos^2\theta + (B^N)^2 \sin^2\theta \qquad (9)$$

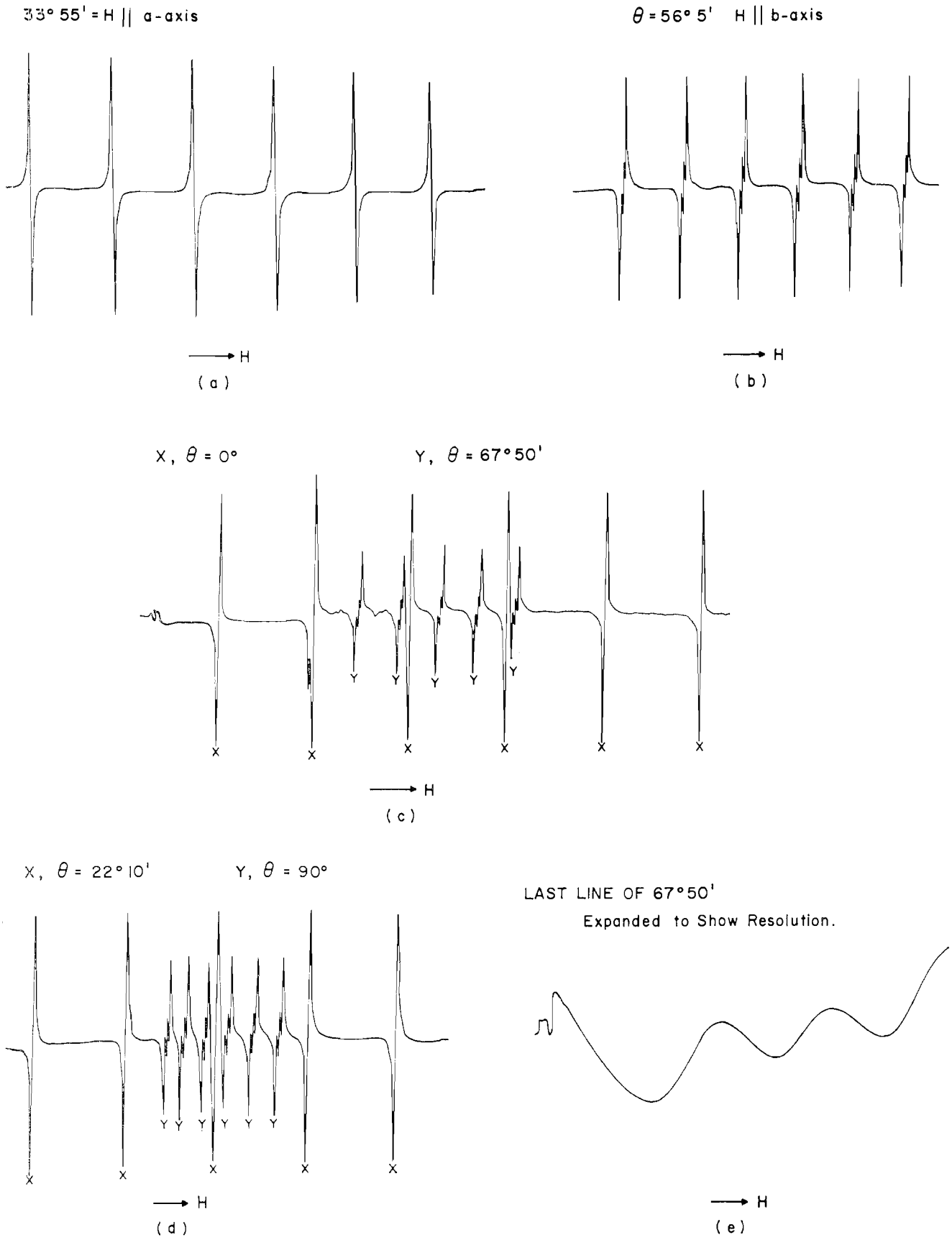

Figure 2.—(a) Esr spectrum of $Mn(CN)_5NO^{2-}$. Applied field H parallel to the a axis. (b) Esr spectrum of $Mn(CN)_5NO^{2-}$. Applied field H parallel to the b axis. (c) Esr spectrum of $Mn(CN)_5NO^{2-}$. Applied field H parallel to one of the NC–Fe–NO axes. (d) Esr spectrum of $Mn(CN)_5NO^{2-}$. Applied field H perpendicular to one of the NC–Fe–NO axes. (e) One of the nitrogen triplets at $\theta = 67° 50'$.

TABLE I

ELECTRON SPIN RESONANCE RESULTS FOR $Mn(CN)_5NO^{2-}$ AND $Cr(CN)_5NO^{3-}$ IN SINGLE CRYSTALS (A VALUES IN GAUSS)

	$Mn(CN)_5NO^{2-}$ [a]	$Cr(CN)_5NO^{3-}$ [b]
$g_{\|\|}$	1.9922	1.9722
$g_\perp$	2.0311	2.0045
g_{av}	2.0181	1.9937
$A_{\|\|}$ (^{55}Mn or ^{53}Cr)	159.98	33.4
$A_\perp$ (^{55}Mn or ^{53}Cr)	36.6	11.9
A_{av}	77.72	19.1
$A_{\|\|}$ (^{14}N)	1.91	2.89
$A_\perp$ (^{14}N)	4.75	7.10
A_{av} (^{14}N)	3.80[c]	5.70[c]
$A_{\|\|}$ (^{13}C)		9.35
$A_\perp$ (^{13}C)		12.95

[a] The g and A values were corrected by solving the spin Hamiltonians to second order; see ref 16. [b] From ref 8. [c] Calculated from $A_{\|\|}$ and $A_\perp$; solution value for $Cr(CN)_5NO^{3-}$ is 5.32 gauss (ref 8).

In eq 9, A_θ^N is the splitting constant for nitrogen at some orientation θ, where it could be measured from the experimental spectrum accurately. B^N also represents an accurate experimental value since it was measured from a well-resolved spectrum. Using the values of A_θ^N, obtained at different orientations θ, and the value for B^N, several values for A^N were calculated. The calculated A^N values are all equal to 1.91 ± 0.02 gauss; thus we take $A^N = 1.91$ gauss. The g_{av} and A_{av} were calculated using the equations

$$\begin{aligned} g_{av} &= 1/3(g_{\|} + 2g_\perp) \\ A^N{}_{av} &= 1/3(A^N + 2B^N) \\ A^{Mn}{}_{av} &= 1/3(A^{Mn} + 2B^{Mn}) \end{aligned} \tag{10}$$

These calculated values are given in Table I. The experimental g values and the hyperfine splitting constants were found to fit the equations

$$\begin{aligned} g^2 &= g_{\|}{}^2 \cos^2\theta + g_\perp{}^2 \sin^2\theta \\ K^2 &= A^2 \cos^2\theta + B^2 \sin^2\theta \end{aligned} \tag{11}$$

Molecular Orbitals for $M(CN)_5NO^{n-}$ Complexes.—Following the method used[2] in the calculation of $Fe(CN)_5NO^{2-}$, detailed SCCC–MO calculations have been carried out for the $M(CN)_5NO^{n-}$ complexes with M = V (n = 5), M = Cr (n = 3), and M = Mn (n = 3, 2). The coordinate system shown in Figure 3 was assumed in all cases. The bond distances[17] in $Fe(CN)_5NO^{2-}$ have been taken for the other complexes to calculate the overlap integrals. Radial functions for the metals V, Cr, and Mn are those of Richardson, *et al.*[18] All other details of the calculations are the same as those in the model system $Fe(CN)_5NO^{2-}$.[2]

The energy levels previously reported[2] for $Fe(CN)_5NO^{2-}$ are shown in Figure 4. The calculated orderings of the one-electron MO energy levels in the several $M(CN)_5NO^{n-}$ complexes are similar to the ordering for $Fe(CN)_5NO^{2-}$. The part of the energy level scheme needed for the assignment of the electronic spectra

(17) P. T. Manoharan and W. C. Hamilton, *Inorg. Chem.*, **2**, 1043 (1963).
(18) J. W. Richardson, W. C. Nieuwport, R. R. Powell, and W. F. Edgell, *J. Chem. Phys.*, **36**, 1057 (1962); *ibid.*, **38**, 796 (1963).

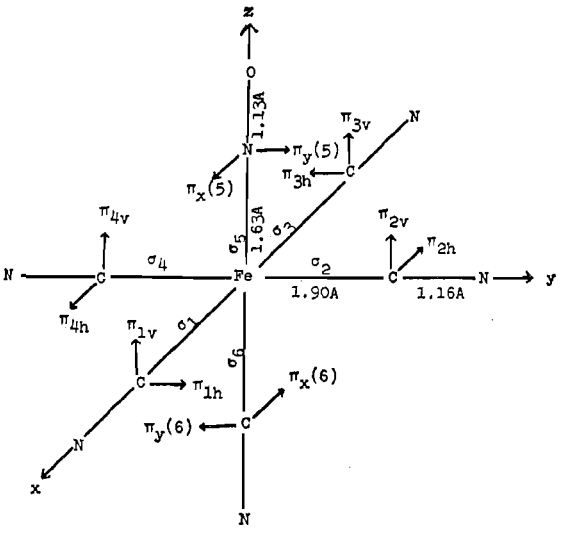

Figure 3.—The structure of $Fe(CN)_5NO^{2-}$ and coordinate system for molecular orbitals.

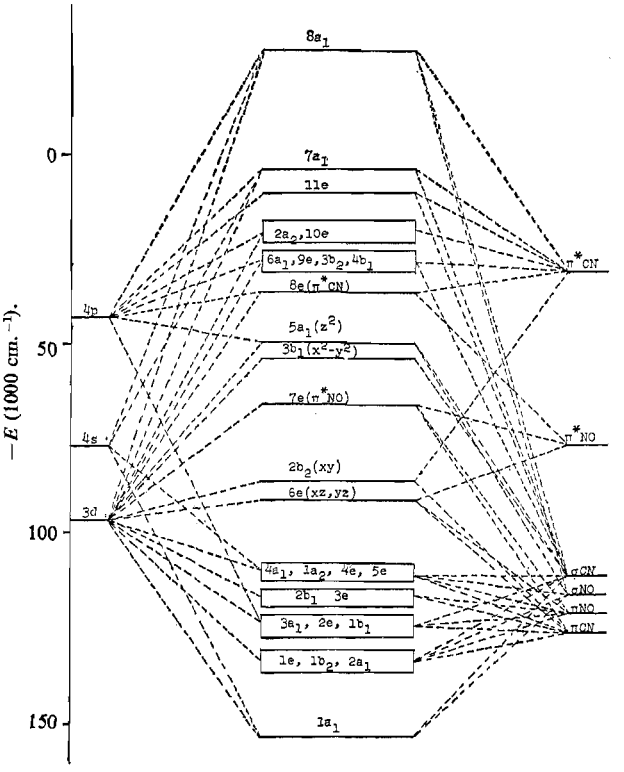

Figure 4.—Molecular orbital energy levels for $Fe(CN)_5NO^{2-}$.

of these complexes in most cases is identical with that for $Fe(CN)_5NO^{2-}$, namely $6e < 2b_2 < 7e < 3b_1 < 5a_1 < 8e$. However, for $Cr(CN)_5NO^{3-}$, the calculated energy level scheme places the $3b_1(x^2 - y^2)$ and $5a_1$ (z^2) levels at almost the same energy, and for $V(CN)_5NO^{5-}$ we have $5a_1(z^2) < 3b_1(x^2 - y^2)$.

Another interesting difference in the complexes is in the composition of the 6e and 7e levels. Population analysis results in Table II reveal this behavior. In general, the metal d_{xz},d_{yz} character in the 6e level and the π^*NO character in the 7e level decrease in going from $Fe(CN)_5NO^{2-}$ to $V(CN)_5NO^{5-}$. Specifically, for $Mn(CN)_5NO^{3-, 2-}$ and $Fe(CN)_5NO^{2-}$ the 6e level

TABLE II

POPULATION ANALYSIS (IN %) OF $2b_2$, 6e, AND 7e LEVELS OF $M(CN)_5NO^{n-}$ COMPLEXES

MO level	Orbital	V (n = 5)	Cr (n = 3)	Mn (n = 2)	Mn (n = 3)	Fe (n = 2)
$2b_2$	π^*CN	21.00	8.24	3.64	4.7	1.58
6e	xz,yz	20.48	38.05	52.19	46.63	60.71
	π^*NO	73.68	50.18	32.80	42.22	24.79
7e	xz,yz	52.77	40.75	27.73	37.09	22.90
	π^*NO	21.71	45.97	64.96	54.84	72.53

is mainly d_{xz},d_{yz}, whereas it has mainly π^*NO character in the $V(CN)_5NO^{5-}$ and $Cr(CN)_5NO^{3-}$ complexes. Similarly, the 7e level is mainly π^*NO for $Mn(CN)_5NO^{3-,2-}$ and $Fe(CN)_5NO^{2-}$, and mainly d_{xz},d_{yz} for $V(CN)_5NO^{5-}$. The $Cr(CN)_5NO^{3-}$ complex represents an intermediate case in which the 7e level has nearly equal π^*NO and d_{xz},d_{yz} character, although the former slightly predominates.

Ground-State Structures.—Table III gives the orderings of the important "spectroscopic" MO levels, the formal electronic configurations, and the ground states of various metal pentacyanonitrosyls. There are two limiting formalisms for the electronic structure of the complexes, depending on the composition of the 6e level, which is fully occupied in all the metal pentacyanonitrosyls. If the 6e level is mainly metal d_{xz},d_{yz}, it is a better approximation to say that the nitric oxide is coordinated as NO^+, with strong π bonding formally of the M→NO^+ type. On the other hand, if the 6e level is predominantly π^*NO, it is better to say that the nitric oxide is coordinated as NO^{3-}, with strong π bonding formally of the NO^{3-}→M type. Of course, we anticipate many cases in which the 6e level is so thoroughly delocalized over d_{xz},d_{yz} and π^*NO that neither formalism is useful. In these cases only a general MO structure can be offered. On the basis of these remarks, $V(CN)_5NO^{5-}$, with over 70% π^*NO character in the 6e level, is assigned the formal electronic configuration $(\pi^*NO)^4d^2$ or d^2NO^{3-} and $Fe(CN)_5NO^{2-}$, with less than 25% π^*NO in 6e, is assigned the formal electronic configuration d^6NO^+.

Recall that we have assumed the bond distances observed for $Fe(CN)_5NO^{2-}$ to calculate the overlap values. In the case of $V(CN)_5NO^{5-}$ and to a lesser extent for $Cr(CN)_5NO^{3-}$, the metal–nitrogen and the metal–carbon distances may be somewhat longer than the ones assumed for the calculations. If this were corrected it would result in less π^*NO character in the occupied 6e levels of these two complexes. However, the unusually large π^*NO contribution in the occupied 6e level indicates that the structure $(\pi^*NO)^4d^2$ represents a much better limiting formalism than the "d^6" assignment for $V(CN)_5NO^{5-}$. In the case of $Cr(CN)_5NO^{3-}$, a clear choice between the limiting formalisms $(\pi^*NO)^4d^1$ and d^5 is difficult to make and we suggest that in this complex reference simply be made to the general MO structure...$(6e)^4(2b_2)^1 = {}^2B_2$. The calculated ground states $^1A_1$ and $^2B_2$ for $V(CN)_5NO^{5-}$ and $Cr(CN)_5NO^{3-}$, respectively, are consistent with the magnetic properties of these complexes.

We may expect that the bond lengths in $Mn(CN)_5NO^{2-,3-}$ will be quite similar to those in $Fe(CN)_5NO^{2-}$, which were used for the energy level calculations. Therefore, we expect the calculated MO energy levels and the population analyses to be reasonably reliable. For $Mn(CN)_5NO^{3-}$ and $Mn(CN)_5NO^{2-}$, the respective ground states $^1A_1$ and $^2B_2$ predicted by the calculation are consistent with their magnetic behavior. In each of these complexes, the 6e level, although principally d_{xz},d_{yz}, has a considerable contribution from the π^*NO level, indicating a formal assignment of coordinated NO^+ with a substantial amount of M→NO^+ π bonding.

TABLE III

ELECTRONIC CONFIGURATIONS FOR METAL PENTACYANONITROSYL COMPLEXES

Complex	Ordering of MO levels[a]	MO structure	Formal structure	Ground state
$Fe(CN)_5NO^{2-}$	$6e(xz,yz) < 2b_2(xy) < 7e(\pi^*NO) < 3b_1(x^2-y^2) < 5a_1(z^2) < 8e(\pi^*CN)$	$(6e)^4(2b_2)^2$	d^6	$^1A_1$
$Mn(CN)_5NO^{3-}$	Same as $Fe(CN)_5NO^{2-}$	$(6e)^4(2b_2)^2$	d^6	$^1A_1$
$Mn(CN)_5NO^{2-}$	Same as $Fe(CN)_5NO^{2-}$	$(6e)^4(2b_2)^1$	d^5	$^2B_2$
$Cr(CN)_5NO^{3-}$	$6e(\pi^*NO) < 2b_2(xy) < 7e\ (xz,yz) < 3b_1(x^2-y^2) \approx 5a_1(z^2) < 8e(\pi^*CN)$	$(6e)^4(2b_2)^1$	d^6 or $(\pi^*NO)^4d^1$	$^2B_2$
$V(CN)_5NO^{5-}$	$6e(\pi^*NO) < 2b_2(xy) < 7e(xz,yz) < 5a_1(z^2) < 3b_1(x^2-y^2) < 8e(\pi^*CN)$	$(6e)^4(2b_2)^2$	$(\pi^*NO)^4d^2$ better than d^6	$^1A_1$

[a] The levels which are needed for the assignments of various electronic absorption bands are indicated. The valence orbitals which are the principal components of the MO levels are shown in parentheses.

Infrared Spectral Results.—Any reasonable theory of bonding in nitric oxide complexes must be able to account for the gross features of their infrared spectra.[12,13,19,20] To help in understanding the nature of bonding in metal pentacyanonitrosyls, we shall examine the stretching frequencies of N–O, C–N, M–N, and M–C. Table IV gives our assignments of these stretching frequencies for all the $M(CN)_5NO^{n-}$ complexes. The N–O and C–N stretching frequencies occur in the relatively high-energy region. It is no-

(19) G. P. Bor, *J. Inorg. Nucl. Chem.*, **17**, 174 (1961).
(20) P. Gans, *Chem. Commun.* (London), 144 (1965).

TABLE IV

INFRARED STRETCHING FREQUENCIES IN $M(CN)_5NO^{n-}$ COMPLEXES

Complex	Stretching frequencies,[a] cm^{-1} N–O	C–N	M–N	M–C[b]
$Fe(CN)_5NO^{2-}$	1939 ± 1[c] (1900)	2173.4, 2161.6, 2156.7, 2143.4[c]	662.5	417, 425, 433
$Mn(CN)_5NO^{3-}$	1725 ± 5[d] (1710)	2100, 2060,[d] 2138 ± 10 (2105, 2080)	655	368.5, 417.5, 426.0
$Mn(CN)_5NO^{2-}$	1885 ± 5[d]	~2150, 2100[d]	622.5	344.5, 386.5, 391.6
$Cr(CN)_5NO^{3-}$	1645[e] (1645)	2137, 2095[e] (2105, 2080)	618.5	364.5, 402.0, 430
$V(CN)_5NO^{5-}$	1575[f]	2095[f]	[g]	[g]

[a] Values given in parentheses are for the tetrabutylammonium salts in $CHCl_3$. [b] The assignment of these bands as M–C stretching frequencies assumes that the M–C–N bending frequencies are at slightly lower wavenumbers. This is admittedly a risky assumption to make, because in one thoroughly investigated system, $KAu(CN)_2Cl_2$ [L. H. Jones, *Inorg. Chem.*, **4**, 1472 (1965)], the M–C–N bending modes are at slightly higher frequencies than the M–C stretching motions. In the present case, however, assuming that the values quoted for M–C stretching modes are actually due to M–C–N bending motions places the M–C stretching values at wavenumbers much too low to be compatible with the M–N stretching values, which are above 600 cm^{-1}. Obviously, more detailed work in this area is needed. [c] Ref 19. [d] Ref 13. [e] Ref 12b. [f] Ref 12a. [g] Not measured.

table that the C–N stretching frequencies do not show any substantial change from case to case, whereas a large variation in the N–O stretching frequencies is observed. This can be understood in terms of our model, which includes the principal M≡NO link, by recalling that M→NO π bonding varies quite substantially in these complexes. Such M→NO π bonding accommodates some of the negative charge which would otherwise accumulate on the central metal as a result of σ bonding. Furthermore, we expect CN^- to be a poorer π acceptor than NO (or NO^+) because the π^*NO ($-74{,}000$ cm^{-1}) level is considerably more stable than the π^*CN ($-30{,}000$ cm^{-1}) level.[2] Obviously, electrons are more easily accommodated in π^*NO than in π^*CN.

The small change in the C–N stretching frequencies of several metal pentacyanonitrosyls, therefore, is consistent with a relatively small involvement of the π^*CN level in the M–C–N systems. Table II gives the population analysis of the $2b_2$ MO level, which is either singly or doubly occupied in the $M(CN)_5NO^{n-}$ complexes. We see that the electron density associated with π^*CN in most cases is relatively small and probably is insufficient to affect substantially the C–N stretching frequencies. Only in $V(CN)_5NO^{5-}$ does the $2b_2$ level have substantial π^*CN population (21%). Consistently, this complex exhibits a low C–N stretching frequency (2095 cm^{-1}) compared to the values of 2173.4, 2161.6, 2156.7, and 2143.4 cm^{-1} for $Fe(CN)_5NO^{2-}$.

The large decrease in the N–O stretching frequency in going from M = Fe to V can be correlated with increasing M→π^*NO intramolecular transfer of electronic density. A more quantitative correlation may be made by examining the population analysis of the 6e level. The $M(CN)_5NO^{n-}$ ions have fully occupied 6e levels. As the π^*NO character of the 6e level increases, the value of the N–O stretching frequency decreases, as shown in Table V.

An attempt has been made to locate the M–N and M–C stretching frequencies in the low-frequency infrared spectra of the $M(CN)_5NO^{n-}$ complexes, using the well-documented assignments[21] for the $Co(CO)_3NO$ complex as a guide. Considerable difficulties were encountered in locating these vibrational frequencies because of the presence of librational modes due to water and the deformation modes of M–N–O and M–C–N. Thus it is only possible to make tentative assignments at this time. The M–N stretching and the N–O bending modes are assigned to the two bands found at ~600 cm^{-1}. There are a large number of bands in the 250–500 cm^{-1} region, assignable to M–C stretching and M–C–N and M–N–O rocking modes. The C–M–C and C–M–N rocking modes can be ignored because they should occur at very low frequencies, perhaps 80 cm^{-1}.[22] It is also reasonable to expect the M–C stretching vibrations to occur at higher energies than the M–C–N bending vibrations. Thus the high-energy peaks are assigned to M–C stretches and the low-energy peaks to M–C–N bending vibrations.

TABLE V

Complex	N–O str frequency, cm^{-1}	% π^*NO character of the 6e level
$Fe(CN)_5NO^{2-}$	1939	24.79
$Mn(CN)_5NO^{2-}$	1885	31.80
$Mn(CN)_5NO^{3-}$	1725	42.22
$Cr(CN)_5NO^{3-}$	1645	50.18
$V(CN)_5NO^{5-}$	1575	73.68

A detailed comparison of the M–C or M–N stretching frequencies observed in the several complexes will not be attempted due to the tentative nature of the assignments. However, it is clear that the simple conclusion that can be extracted from these spectra is that the M–N bond is considerably "stiffer" than any of the M–C bonds, as we have continually emphasized in our electronic structural model.

Electronic Spectra.—It is important to establish the main similarities and differences in the electronic spec-

(21) R. S. McDowell, W. D. Horrocks, Jr., and J. T. Yates, *J. Chem. Phys.*, **34**, 530 (1961).

(22) K. Nakamoto, "Infrared Spectra of Inorganic and Coordination Compounds," John Wiley and Sons, New York, N. Y., 1963, pp 146–151, 169–172.

tra of isoelectronic metal pentacyanonitrosyls and to relate these spectral comparisons to the nature of the M–NO bonding in the complexes. In making the electronic spectral assignments, we shall follow the derived molecular orbital energy level scheme and use as a guide the well-established assignments[2] of the electronic spectrum of $Fe(CN)_5NO^{2-}$. Thus we shall first review the spectrum of $Fe(CN)_5NO^{2-}$.

$Fe(CN)_5NO^{2-}$.—The assignments of the electronic spectrum of $Fe(CN)_5NO^{2-}$ have been discussed in detail in a previous paper.[2] These spectral assignments are summarized in Table VI. The bands at 20,080 and 25,380 cm^{-1} are polarized x,y and z, respectively, consistent with the assignments $^1A_1 \rightarrow {}^1E(2b_2 \rightarrow 7e)$ and $^1A_1 \rightarrow {}^1A_1(6e \rightarrow 7e)$. Low-temperature experiments have established the orbitally-allowed nature of these two bands. The aqueous solution bands at 30,300, 37,800, and 42,000 cm^{-1} are assigned as d–d type bands, whereas the intense 50,000 cm^{-1} band is assigned as the metal$\rightarrow\pi^*$CN transition $^1A_1 \rightarrow {}^1E$ $(2b_2 \rightarrow 8e)$.

TABLE VI

ELECTRONIC SPECTRUM OF $Fe(CN)_5NO^{2-}$ (ENERGIES IN cm^{-1})

Obsd maxima and polarizations[a]	ϵ_{max}	Calcd energies and polarizations	Band assignments
20,080 ($\perp$)	*ca.* 8	20,540 ($\perp$)	$^1A_1 \rightarrow {}^1E(2b_2 \rightarrow 7e)$
25,380 ($\parallel$)	25	25,090 ($\parallel$)	$^1A_1 \rightarrow {}^1A_1(6e \rightarrow 7e)$
(30,300)[b] ($\perp$)	(40)[b]	30,770[c] (vibronic $\perp$)	$^1A_1 \rightarrow {}^1A_2(2b_2 \rightarrow 3b_1)$
(37,800)[b]	(900)[b]	37,750[c] ($\perp$)	$^1A_1 \rightarrow {}^1E(6e \rightarrow 5a_1)$
(42,000)[b]	(700)[b]	40,900[c] ($\perp$)	$^1A_1 \rightarrow {}^1E(6e \rightarrow 3b_1)$
50,000	24,000	49,900 ($\perp$)	$^1A_1 \rightarrow {}^1E(2b_2 \rightarrow 8e)$

[a] Maxima for an aqueous solution spectrum of $Na_2Fe(CN)_5NO\cdot 2H_2O$. Polarizations from the single crystal spectra. [b] Shoulder, ϵ_{max} values are estimates. [c] Corrected for inter-electronic-repulsion energy, assuming $F_2 = 10F_4$. The Slater–Condon parameters are from ref 6. The value of $(F_2 - 5F_4) = 400$ cm^{-1} from the $Fe(CN)_6^{4-}$ spectrum was assumed for $Fe(CN)_5NO^{2-}$. Configuration interaction between the two closely-spaced ^1E states was included.

We have now extended our detailed low-temperature and polarized-spectral results[2] to include the third band in the spectrum of $Fe(CN)_5NO^{2-}$, which in aqueous solution appears as a shoulder at 30,300 cm^{-1}. Spectra of $[(n\text{-}C_4H_9)_4N]_2[Fe(CN)_5NO]$ in EPA solutions at room and liquid nitrogen temperatures are shown in Figure 5. The intensity in the region of 30,300 cm^{-1} is reduced at liquid nitrogen temperature. Moreover, at the low temperature, the band separates into two well-resolved peaks at 28,818 and 30,960 cm^{-1}, or a separation of 2142 cm^{-1}. The transition $^1A_1 \rightarrow {}^1A_2$ is orbitally forbidden because the product A_1A_2 does not include the symmetry of the electric dipole vector and therefore the electronic transition moment integral is zero. However, if the electronic transition occurs with the simultaneous excitation of a vibration of E symmetry, the total wave function for the excited state will be of E symmetry and the transition will be allowed in x,y polarization. The 2142 cm^{-1} separation of two well-resolved components of the third band may be considered to represent the degenerate E(C–N) stretching frequency of $Fe(CN)_5NO^{2-}$ in the excited electronic state. The reported frequencies for the E mode in the ground state from the well-resolved spectrum of $Fe(CN)_5NO^{2-}$ ion are 2161.6 and 2156.7 cm^{-1}.[19] The value 2142 cm^{-1} for the excited electronic state is not appreciably different from the ground-state values. We conclude that the $^1A_1 \rightarrow {}^1A_2$ transition is allowed when there is a simultaneous excitation of an E symmetry stretching motion. The single crystal spectra of $Na_2Fe(CN)_5NO\cdot 2H_2O$ using polarized light reveal the position of the maximum of the $^1A_1 \rightarrow {}^1A_2$ band to be 30,490 cm^{-1}, as shown in Figure 6. Moreover, the band is $\perp$ or x,y polarized, consistent with a model in which the perturbing vibration is of E symmetry. Thus the combined polarized-single-crystal and low-temperature spectra establish that the transition at 30,300 cm^{-1} in aqueous solution is $^1A_1 \rightarrow {}^1A_2$, vibronically allowed by doubly degenerate stretching motions.

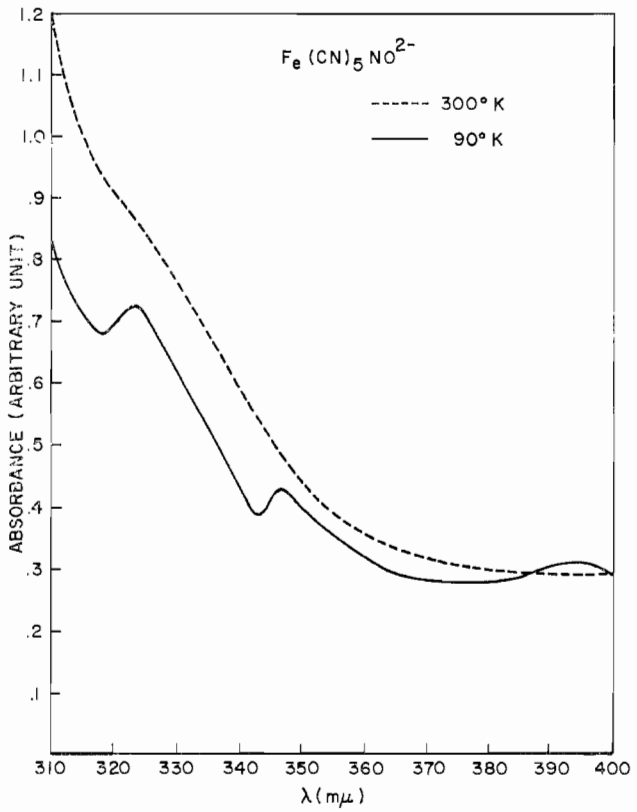

Figure 5.—Electronic spectra of $[(n\text{-}C_4H_9)_4N]_2[Fe(CN)_5NO]$ in EPA solution: dashed curve, 6.75×10^{-3} M solution at 300°K; solid curve, 6.75×10^{-3} M frozen solution at 77°K; 0.6-cm path length.

$Mn(CN)_5NO^{3-}$ and $V(CN)_5NO^{5-}$.—The ions $Mn(CN)_5NO^{3-}$ and $V(CN)_5NO^{5-}$ are isoelectronic with $Fe(CN)_5NO^{2-}$. The spectra of these complexes in aqueous solution are reported and assigned in Table VII. Room- and low-temperature spectra in EPA solution are given in Table VIII. The electronic spectrum of $Mn(CN)_5NO^{3-}$ in aqueous solution exhibits bands with maxima at 18,520 (ϵ 22.2), 28,980 (ϵ 111.4), 42,550 (ϵ ~4500), and 45,450 cm^{-1} (ϵ ~5000). There is also a

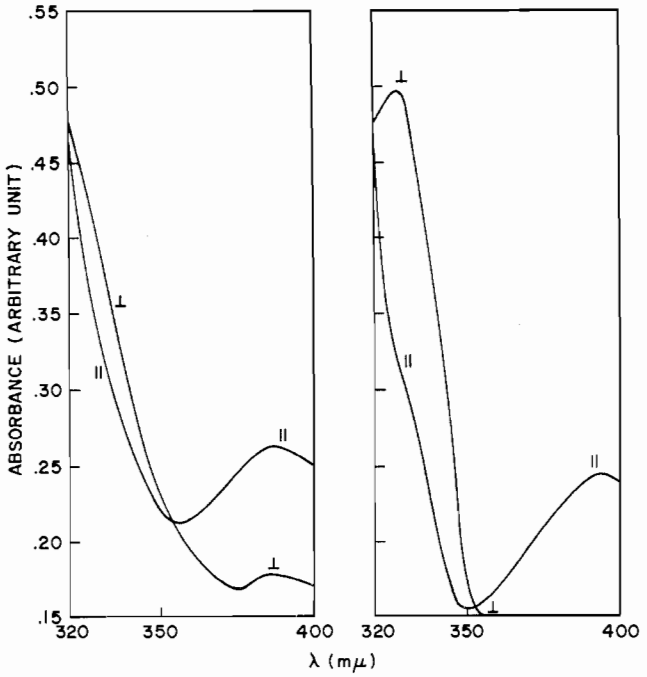

Figure 6.—Measured and calculated spectra of $Na_2Fe(CN)_5NO\cdot 2H_2O$ using polarized light in the region 400–320 mμ: right curve, calculated spectra ∥ and ⊥ to optically equivalent Fe–NO axes; left curve, measured spectra ∥ and ⊥ to the *a* axis.

TABLE VII
ELECTRONIC SPECTRA OF $M(CN)_5NO^{n-}$ COMPLEXES IN AQUEOUS SOLUTION

Complex	Obsd maxima, cm^{-1}	ϵ_{max}	Calcd energies, cm^{-1}	Band assignments
$Mn(CN)_5NO^{3-}$	18,520	22.2	14,700	$^1A_1 \rightarrow {}^1E(2b_2 \rightarrow 7e)$
	~24,690	~66[a]	24,200	$^1A_1 \rightarrow {}^1A_1(6e \rightarrow 7e)$
	28,980	111.4	26,500[b]	$^1A_1 \rightarrow {}^1A_2(2b_2 \rightarrow 3b_1)$
	37,850	~1000	37,770[c]	$^1A_1 \rightarrow {}^1E(6e \rightarrow 5a_1)$
	42,550	~4500	41,490[c]	$^1A_1 \rightarrow {}^1E(6e \rightarrow 3b_1)$
	45,450	~5000	40,470	$^1A_1 \rightarrow {}^1E(2b_2 \rightarrow 8e)$
$V(CN)_5NO^{5-}$	12,900	1.15	9,200	$^1A_1 \rightarrow {}^1E(2b_2 \rightarrow 7e)$
	21,160	36.5	19,000[b]	$^1A_1 \rightarrow {}^1A_2(2b_2 \rightarrow 3b_1)$
	32,470	~1000	30,100	$^1A_1 \rightarrow {}^1A_1(6e \rightarrow 7e)$
	37,470	5200	23,260	$^1A_1 \rightarrow {}^1E(2b_2 \rightarrow 8e)$
$Cr(CN)_5NO^{3-}$	13,700	8	12,660	$^2B_2 \rightarrow {}^2E(6e \rightarrow 2b_2)$
	15,380	~1.5	13,890	$^2B_2 \rightarrow {}^2E(2b_2 \rightarrow 7e)$
	22,200	72	26,550	$^2B_2 \rightarrow {}^2B_2(6e \rightarrow 7e)$
	27,320	59	28,260	$^2B_2 \rightarrow {}^2B_1(2b_2 \rightarrow 3b_1)$
	37,300	1100	37,420	$^2B_2 \rightarrow {}^2E(5e \rightarrow 3b_2)$
	43,480	3600	35,680	$^2B_2 \rightarrow {}^2E(2b_2 \rightarrow 8e)$
$Mn(CN)_5NO^{2-}$	12,050	19	7,820	$^2B_2 \rightarrow {}^2E(6e \rightarrow 2b_2)$
	18,600	~20	18,350	$^2B_2 \rightarrow {}^2E(2b_2 \rightarrow 7e)$
	25,960	1700	26,170	$^2B_2 \rightarrow {}^2B_2(6e \rightarrow 7e)$
	28,570	120	32,530	$^2B_2 \rightarrow {}^2B_1(2b_2 \rightarrow 3b_1)$
	32,280	880	28,830	$^2B_2 \rightarrow {}^2E(5e \rightarrow 2b_2)$
	37,030	2400	38,740	$^2B_2 \rightarrow {}^2E(6e \rightarrow 5a_1)$
	48,540	23,800	45,050	$^2B_2 \rightarrow {}^2E(2b_2 \rightarrow 8e)$

[a] ϵ_{max} was estimated from relative peak heights in the low-temperature spectrum in a frozen EPA solution; see Table VIII. [b] Corrected for interelectronic-repulsion energy, assuming $F_2 = 10F_4$. The Slater–Condon parameters are from ref 6. The value of $(F_2 - 5F_4) = 400$ cm^{-1} from the $Fe(CN)_6^{4-}$ spectrum was assumed for $M(CN)_5NO^{n-}$. [c] Configuration interaction between the two closely spaced ^1E states was included.

shoulder at 37,850 cm^{-1} (ϵ ~1000). The band containing the 42,550 and 45,450 cm^{-1} maxima is very broad and thus the two peaks are not well resolved. All five bands are too intense to be spin-forbidden and so we shall immediately designate them as due to spin-allowed transitions.

TABLE VIII
ELECTRONIC SPECTRA OF $[(n\text{-}C_4H_9)_4N]_m[M(CN)_5NO]$ COMPLEXES IN EPA SOLUTION (ENERGIES IN cm^{-1})

Complex ion	Absorption max at room temp	Absorption max at low temp	Intensity change at low temp
$Fe(CN)_5NO^{2-}$	18,650	18,650	No change
	25,380	25,380	Slight increase
	30,300	28,818	Decreases with peak separation of 2142 cm^{-1}
		30,960	
$Mn(CN)_5NO^{3-}$	18,010	18,510	No change
	...	24,690	New shoulder appears
	28,570	29,150	Decreases
$Cr(CN)_5NO^{3-}$	14,390	13,990	No change
	22,220	19,324	Slight increase with peak separations of 566, 507, 468, 468, 465, 362 cm^{-1}
		19,890	
		20,397	
		20,865	
		21,333	
		21,798	
		22,160	
$Mn(CN)_5NO^{2-}$	25,310	25,100	Increases
	27,320	27,320	Increases
	31,250	31,250	Increases

Two earlier attempts[6,7] at the assignment of the electronic spectrum of $Mn(CN)_5NO^{3-}$ are now inadequate because they did not consider the low-energy charge-transfer transitions arising from excitations from the 6e and $2b_2$ levels to the relatively stable 7e (π^*NO) level. We assign the bands at 18,520 and 28,980 cm^{-1} as the electronic transitions $^1A_1 \rightarrow {}^1E$ ($2b_2 \rightarrow 7e$) and $^1A_1 \rightarrow {}^1A_2(2b_2 \rightarrow 3b_1)$, respectively, in analogy to spectral assignments for $Fe(CN)_5NO^{2-}$. The nitroprusside ion has similar bands at 20,080 and 30,300 cm^{-1}, which were assigned to the $^1A_1 \rightarrow {}^1E(2b_2 \rightarrow 7e)$ and $^1A_1 \rightarrow {}^1A_2(2b_2 \rightarrow 3b_1)$ transitions, respectively, on the basis of considerable evidence from low-temperature and single-crystal polarized spectra. Since the complexes $Mn(CN)_5NO^{3-}$ and $Fe(CN)_5NO^{2-}$ are isoelectronic and have similar net charges, they are expected to have these two bands in common. Moreover, we know that the Δ values (separation between the t_{2g} and e_g levels) in octahedral metal cyanides with d^6 electronic configurations decrease in going from Co to Mn as the central metal.[23] Since the bonding situation in the *xy* plane is similar in $M(CN)_6^{n-}$ and $M(CN)_5NO^{n-}$ complexes, the separation of the $2b_2(xy)$ and $3b_1(x^2 - y^2)$ orbitals is expected to decrease in going from $Fe(CN)_5NO^{2-}$ to $V(CN)_5NO^{5-}$.

The energy of a particular charge-transfer transition is expected to decrease as the formal charge of the central metal ion is decreased. The formal charges of the metal ions are 2+ and 1+ in $Fe(CN)_5NO^{2-}$ and $Mn(CN)_5NO^{3-}$. Since the $2b_2 \rightarrow 7e$ transition is essentially M→L charge transfer, it is consistent that the $2b_2 \rightarrow 7e$ transition has lower energy for $Mn(CN)_5NO^{3-}$ than for $Fe(CN)_5NO^{2-}$. The MO calculations are also consistent with lower M→L charge-transfer energies for $Mn(CN)_5NO^{3-}$ than for $Fe(CN)_5NO^{2-}$. Even though the calculated one-electron separation of 14,700 cm^{-1} for the $2b_2 \rightarrow 7e$ transition in $Mn(CN)_5NO^{3-}$ is only in

(23) H. B. Gray and N. A. Beach, *J. Am. Chem. Soc.*, **85**, 2922 (1963).

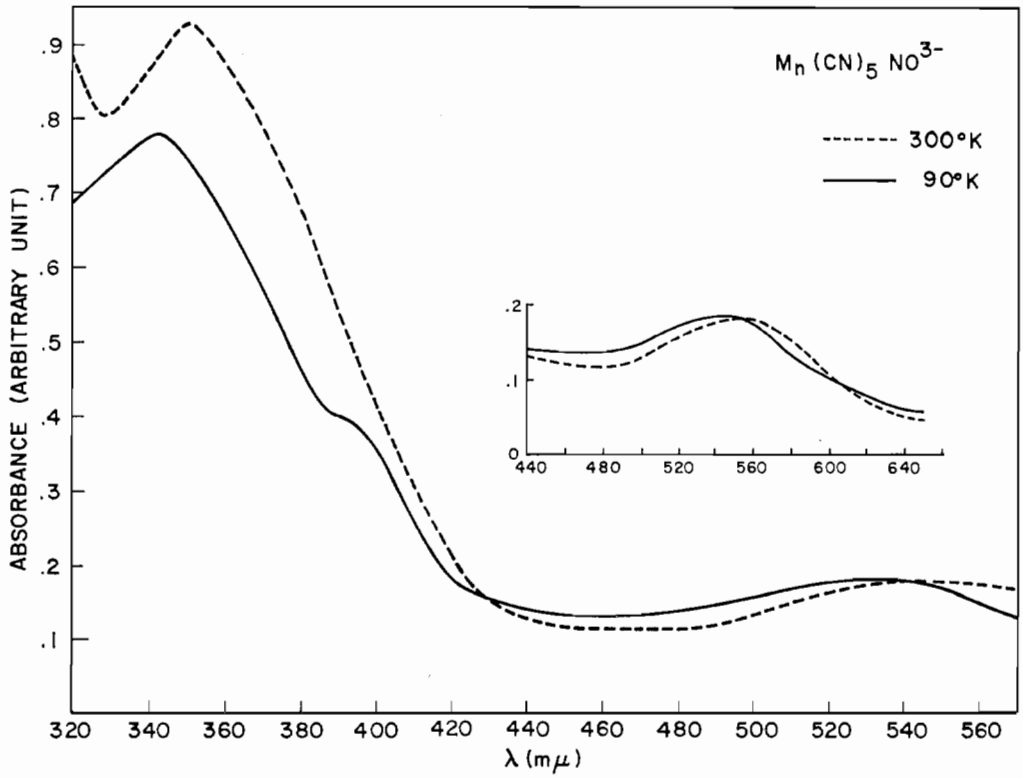

Figure 7.—Electronic spectra of $[(n\text{-}C_4H_9)_4N]_3[Mn(CN)_5NO]$ in EPA solution: dashed curve at 300°K; solid curve at 90°K.

fair agreement with the band maximum, it is clearly smaller than the calculated $2b_2 \rightarrow 7e$ separation in $Fe(CN)_5NO^{2-}$.

Finally, we note that the calculated energy (corrected for interelectronic repulsion) of 26,500 cm^{-1} for the $^1A_1 \rightarrow {}^1A_2(2b_2 \rightarrow 3b_1)$ transition is in moderately good agreement with the spectral value of 28,900 cm^{-1}.

The remaining three bands at 37,850, 42,550, and 45,450 cm^{-1} are assigned to the same transitions as the $Fe(CN)_5NO^{2-}$ bands at 37,800, 42,000, and 50,000 cm^{-1}. Thus, the $Mn(CN)_5NO^{3-}$ bands at 37,850 and 42,550 cm^{-1} are assigned $^1A_1 \rightarrow {}^1E(6e \rightarrow 5a_1)$ and $^1A_1 \rightarrow {}^1E(6e \rightarrow 3b_1)$. The calculated energies of 37,770 and 41,490 cm^{-1}, including corrections for interelectronic repulsion and configuration interaction between the closely spaced ^1E levels, are in very good ageement with the experimental values. The last band, at 45,450 cm^{-1}, is assigned as the metal-to-ligand (π^*CN) charge-transfer transition $^1A_1 \rightarrow {}^1E(2b_2 \rightarrow 8e)$. The most convincing evidence in support of this assignment comes from the fact that in the "d^6" hexacyanides of Co(III) and Fe(II), the metal-to-ligand (π^*CN) charge-transfer bands have energies in the increasing order $Fe(CN)_6^{4-} < Co(CN)_6^{3-}$,[23] since the stability of the metal t_{2g} level must increase in the order Fe(II) < Co(III). The difference between the metal-to-ligand type charge-transfer transition energies in $Fe(CN)_6^{4-}$ and $Co(CN)_6^{3-}$ is 4200 cm^{-1}. We note that for $Mn(CN)_5NO^{3-}$ and $Fe(CN)_5NO^{2-}$, the difference in the energies of the two bands in question is 4550 cm^{-1}, with the Fe(II) band at higher energy. Therefore, we confidently assign the band at 45,450 cm^{-1} in $Mn(CN)_5NO^{3-}$ to the transition $^1A_1 \rightarrow {}^1E(2b_2 \rightarrow 8e)$.

The only difference between the room-temperature spectra of $Fe(CN)_5NO^{2-}$ and $Mn(CN)_5NO^{3-}$ is that a band, similar to the one assigned to the transition $^1A_1 \rightarrow {}^1A_1(6e \rightarrow 7e)$ found at 25,380 cm^{-1} in $Fe(CN)_5NO^{2-}$, is missing in $Mn(CN)_5NO^{3-}$. It is gratifying, however, that in the better resolved low-temperature spectrum of $Mn(CN)_5NO^{3-}$, shown in Figure 7, this band is revealed at 24,690 cm^{-1} as a shoulder. This new band at 24,690 cm^{-1} is assigned as the "missing" $^1A_1 \rightarrow {}^1A_1(6e \rightarrow 7e)$ transition. Also of importance is the fact that at liquid nitrogen temperature the intensity of the band at 28,980 cm^{-1} is decreased, in strong support of our assignment as the orbitally-forbidden transition $^1A_1 \rightarrow {}^1A_2(2b_2 \rightarrow 3b_1)$. Recall that the $^1A_1 \rightarrow {}^1A_2$ band in $Fe(CN)_5NO^{2-}$ shows this type of temperature dependence. It is also worth noting that the molar extinction coefficients for the bands $^1A_1 \rightarrow {}^1E(2b_2 \rightarrow 7e)$, $^1A_1 \rightarrow {}^1A_1(6e \rightarrow 7e)$, and $^1A_1 \rightarrow {}^1A_2(2b_2 \rightarrow 3b_1)$ are approximately in the ratio of 1:3:5 both in $Fe(CN)_5NO^{2-}$ and $Mn(CN)_5NO^{3-}$, at the temperature of liquid nitrogen.

Finally, examination of the three metal-to-ligand (π^*) type charge-transfer transitions $^1A_1 \rightarrow {}^1E(2b_2 \rightarrow 7e)$, $^1A_1 \rightarrow {}^1A_1(6e \rightarrow 7e)$, and $^1A_1 \rightarrow {}^1E(2b_2 \rightarrow 8e)$ of $Fe(CN)_5NO^{2-}$ and $Mn(CN)_5NO^{3-}$ reveals that in every case there is an increase in the energy of a particular charge-transfer transition on increasing the positive charge of the central metal ion (Mn(I) < Fe(II)). This is expected for metal-to-ligand (π^*) transitions and has been used extensively as evidence for the transition type.[24]

The electronic spectrum of $V(CN)_5NO^{5-}$ consists of

(24) H. B. Gray and C. J. Ballhausen, *J. Am. Chem. Soc.*, **85**, 260 (1963).

peaks at 12,900 (ϵ 1.15), 21,160 (ϵ 36.5), and 37,470 cm^{-1} (ϵ 5200) and a shoulder at 32,470 cm^{-1} ($\epsilon \sim 1000$). The first band at 12,900 cm^{-1} is assigned to the transition $^1A_1 \rightarrow {}^1E(2b_2 \rightarrow 7e)$. The very small extinction coefficient of the 12,900 cm^{-1} band probably reflects the large metal d character of both the $2b_2$ and 7e levels in this complex. The calculated energy of 9200 cm^{-1} for $2b_2 \rightarrow 7e$ is in fair agreement with the spectral value of 12,900 cm^{-1}, considering interelectronic-repulsion energy has not been included.

The second band at 21,160 cm^{-1} is assigned as the orbitally-forbidden $^1A_1 \rightarrow {}^1A_2(2b_2 \rightarrow 3b_1)$ transition. The calculated energy of 19,000 cm^{-1}, including an interelectronic-repulsion correction, is in reasonable agreement. Moreover, the $2b_2 \rightarrow 3b_1$ separation is expected to decrease in the order $Fe(CN)_5NO^{2-} > Mn(CN)_5NO^{3-} > V(CN)_5NO^{5-}$, following the decrease in the Δ values of metal hexacyanide complexes. Additional support for this assignment comes from the fact that the "d^2" hexacyanide of vanadium, namely $V(CN)_6^{3-}$, has a Δ value of only 23,600 cm^{-1}.[25] The difference in σ and π bonding which leads to Δ in $V(CN)_6^{3-}$ and that responsible for the $2b_2 \rightarrow 3b_1$ separation in $V(CN)_5NO^{5-}$ should be quite similar. Thus we feel that the assignment $^1A_1 \rightarrow {}^1A_2(2b_2 \rightarrow 2b_1)$ for the transition at 21,160 cm^{-1} is justified.

The shoulder at 32,470 cm^{-1} is assigned to the transition $^1A_1 \rightarrow {}^1A_1(6e \rightarrow 7e)$. Recall that $V(CN)_5NO^{5-}$ has a formal ground-state assignment of $(\pi^*NO)^4d^2$. Thus the $6e \rightarrow 7e$ transition in $V(CN)_5NO^{5-}$ must be regarded as a ligand-to-metal type charge transfer. This is of interest because in $Fe(CN)_5NO^{2-}$ and $Mn(CN)_5NO^{3-}$ the $6e \rightarrow 7e$ transition is formally of the metal-to-ligand charge-transfer type. If the $6e \rightarrow 7e$ transition in $V(CN)_5NO^{5-}$ were a metal-to-ligand charge-transfer transition, it should occur at lower energy than the $6e \rightarrow 7e$ transition energies of 24,690 and 25,380 cm^{-1}, observed for $Mn(CN)_5NO^{3-}$ and $Fe(CN)_5NO^{2-}$, respectively. As further support for the assignment, the calculated orbital energy of 30,100 cm^{-1} is in reasonable agreement with the spectral value. Recall that the predicted energy of the $6e \rightarrow 7e$ transition in $Mn(CN)_5NO^{3-}$ is less than that predicted for $Fe(CN)_5NO^{2-}$. The increase to 30,100 cm^{-1} in the calculated energy of the $6e \rightarrow 7e$ transition in $V(CN)_5NO^{5-}$ reflects the changing nature of the charge-transfer process accompanying the transition $6e \rightarrow 7e$.

The band at 37,470 cm^{-1} is assigned to the transition $^1A_1 \rightarrow {}^1E(2b_2 \rightarrow 8e)$. The assignment is based on the reasonable assumption that the $2b_2 \rightarrow 8e$ transition energy should slowly decrease in going from $Fe(CN)_5NO^{2-}$ to $V(CN)_5NO^{5-}$ and that these bands are generally intense. The corresponding bands in $Fe(CN)_5NO^{2-}$ and $Mn(CN)_5NO^{3-}$ are located at 50,000 and 45,450 cm^{-1}, respectively. It is therefore reasonable to expect this metal-to-ligand (π^*CN) band at about 37,000 cm^{-1} in $V(CN)_5NO^{5-}$. However, the calculated orbital energy of 23,250 cm^{-1} apparently grossly overestimates the shift to a lower energy value. This probably pinpoints a weakness in the calculation, namely the neglect of the effect on the coulomb integrals as negative charge builds up on the ligands. In a complex such as $V(CN)_5NO^{5-}$, the correct value to take for the π^*CN coulomb integral is undoubtedly at energies more positive than the assumed $-30{,}000$ cm^{-1}, due to the substantial negative-charge accumulation on the CN^- ligands. It is noteworthy that the predicted and observed energies for the $2b_2 \rightarrow 8e$ transition in $Fe(CN)_5NO^{2-}$ agree very well, whereas the predicted energy (40,700 cm^{-1}) is approximately 5000 cm^{-1} lower than the observed energy (45,450 cm^{-1}) for the same transition in $Mn(CN)_5NO^{3-}$.

$Cr(CN)_5NO^{3-}$ and $Mn(CN)_5NO^{2-}$.—Let us now consider the electronic spectra of the paramagnetic species $Cr(CN)_5NO^{3-}$ and $Mn(CN)_5NO^{2-}$. The magnetic measurements[12b,13] confirm the presence of one unpaired electron in each case. Our repeated bulk susceptibility measurements on a solid sample of $K_2Mn(CN)_5NO$ give $\mu_{eff} = 1.73$ BM, indicating $S = 1/2$ with no abnormal behavior. Thus the magnetic moment of 0.50 BM reported earlier[13] for solid $K_2Mn(CN)_5NO$ is apparently in error. The ground-state configuration of each complex on the basis of our derived energy level scheme is $\ldots(6e)^4(2b_2)^1 = {}^2B_2$.

The electronic spectra of $Cr(CN)_5NO^{3-}$ and $Mn(CN)_5NO^{2-}$ are more complicated than those of the diamagnetic species discussed earlier. Table VII gives the essential features of the spectra and our suggested band assignments. The aqueous solution spectrum of $Cr(CN)_5NO^{3-}$ has absorption peaks at 13,700 (ϵ 8), 22,200 (ϵ 72), 27,320 (ϵ 59), 37,300 (ϵ 1100), and 43,480 cm^{-1} (ϵ 3600). There is also a very weak shoulder at 15,380 cm^{-1} (ϵ 1.5). The $Mn(CN)_5NO^{2-}$ complex has peaks at 12,050 (ϵ 19), 25,960 (ϵ 1700), 32,280 (ϵ 880), 37,030 (ϵ 2400), and 48,540 cm^{-1} (ϵ 23,800). It also has two weak shoulders, at 18,600 ($\epsilon \sim 20$) and 28,570 cm^{-1} ($\epsilon \sim 120$).

All these bands are too intense to be spin-forbidden and so only spin-allowed transitions will be considered. For a B_2 ground state in C_{4v} symmetry, transitions to B_2 and E excited states are orbitally allowed. Using this fact, we assign the first bands of the $Cr(CN)_5NO^{3-}$ and $Mn(CN)_5NO^{2-}$ complexes, at 13,700 and 12,050 cm^{-1}, respectively, to the "inner" transition $^2B_2 \rightarrow {}^2E(6e \rightarrow 2b_2)$. The calculated values of 12,660 and 7820 cm^{-1} are in fair agreement with the observed values. In both complexes, the bands at 15,380 (Cr) and 18,600 cm^{-1} (Mn) appear as weak shoulders. They are assigned to the $^2B_2 \rightarrow {}^2E(2b_2 \rightarrow 7e)$ transition. The calculated one-electron energies of 13,890 (Cr) and 18,350 cm^{-1} (Mn) are in good agreement with the experimental values. Support for the assignment in the case of $Mn(CN)_5NO^{2-}$ comes from the spectrum of $Mn(CN)_5NO^{3-}$. The $^1A_1 \rightarrow {}^1E(2b_2 \rightarrow 7e)$ transition was assigned to the band at 18,520 cm^{-1} in the diamagnetic species. This energy is comparable to the energy of the $^2B_2 \rightarrow {}^2E(2b_2 \rightarrow 7e)$ transition in the paramagnetic species $Mn(CN)_5NO^{2-}$.

(25) J. R. Perumareddi, A. D. Liehr, and A. W. Adamson, *J. Am. Chem. Soc.*, **85**, 249(1963).

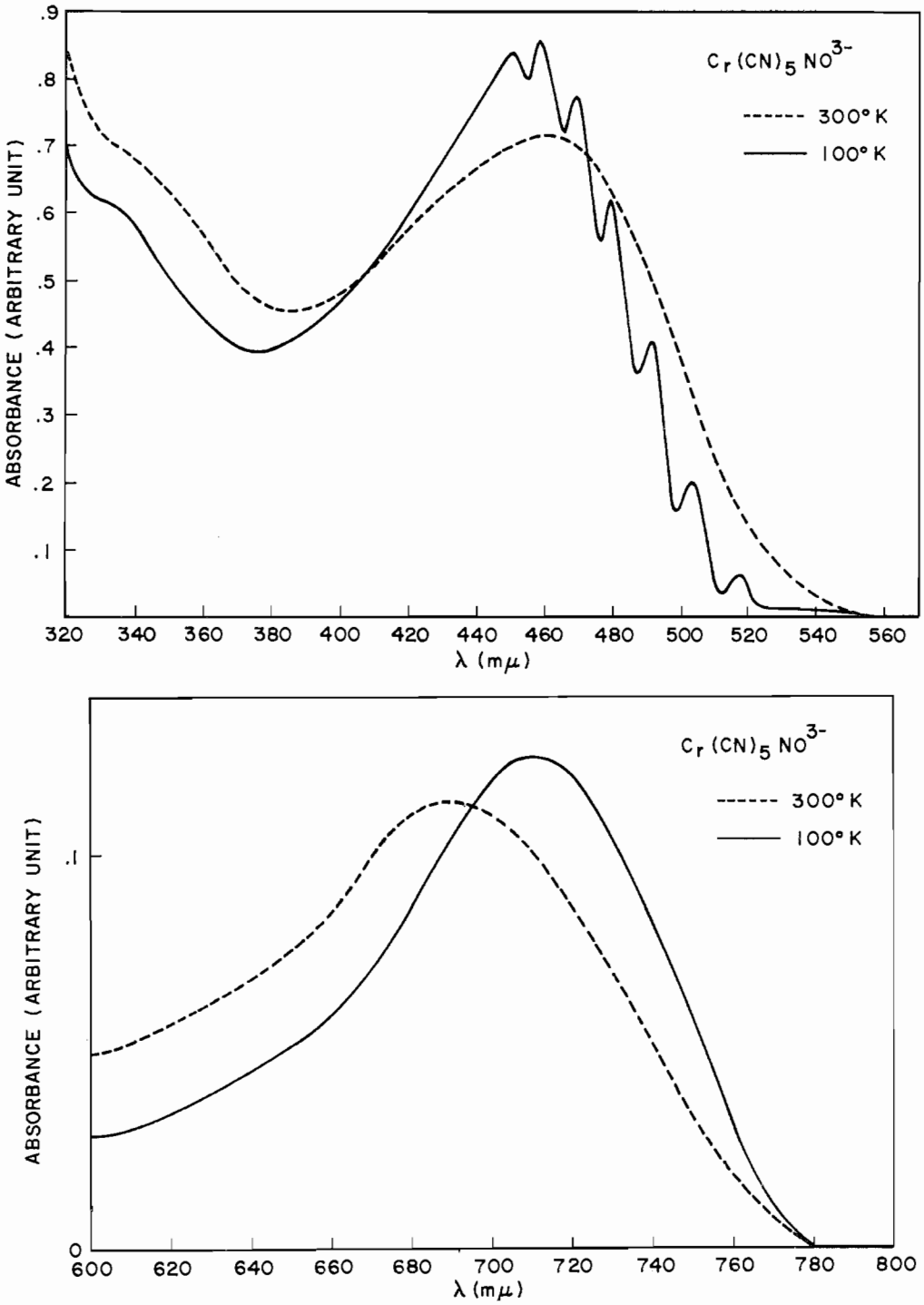

Figure 8.—Electronic spectra of $[(n\text{-}C_4H_9)_4N]_3[Cr(CN)_5NO]$ in EPA solution: dashed curve at 300°K; solid curve at 100°K.

A liquid nitrogen temperature spectral study of both of these complexes is shown in Figures 8 and 9. This study reveals that the intensities of the first two bands in both $Cr(CN)_5NO^{3-}$ and $Mn(CN)_5NO^{2-}$ are not reduced at the low temperature. This indicates the orbitally-allowed nature of the two bands, even though the exact reason for the unusually low extinction coefficient of the band at 15,380 cm^{-1} in $Cr(CN)_5NO^{3-}$ is not known.

The bands at 22,000 cm^{-1} in $Cr(CN)_5NO^{3-}$ and 25,960 cm^{-1} in $Mn(CN)_5NO^{2-}$ are the most interesting of all. They are assigned to the $^2B_2 \rightarrow {}^2B_2(6e \rightarrow 7e)$ transition. Adding the first two transition energies, we have 29,080 and 30,650 cm^{-1}, respectively, for $Cr(CN)_5NO^{3-}$ and $Mn(CN)_5NO^{2-}$. Comparison of these total energies with the energies of the $^2B_2 \rightarrow {}^2B_2$ ($6e \rightarrow 7e$) transitions indicates that there is considerable repulsion relative to the ground state when an electron is excited from the $2b_2$ to the 7e level. In other words, the repulsion energy for the state ^2E—$(6e)^3(7e)^1$—is much greater than that for the state $^2B_2$—$(6e)^3(2b_2)^1(7e)^1$; we may estimate this increased repulsion to be of the order of 6000 cm^{-1}. Because of the relative decrease in interelectronic repulsion on excit-

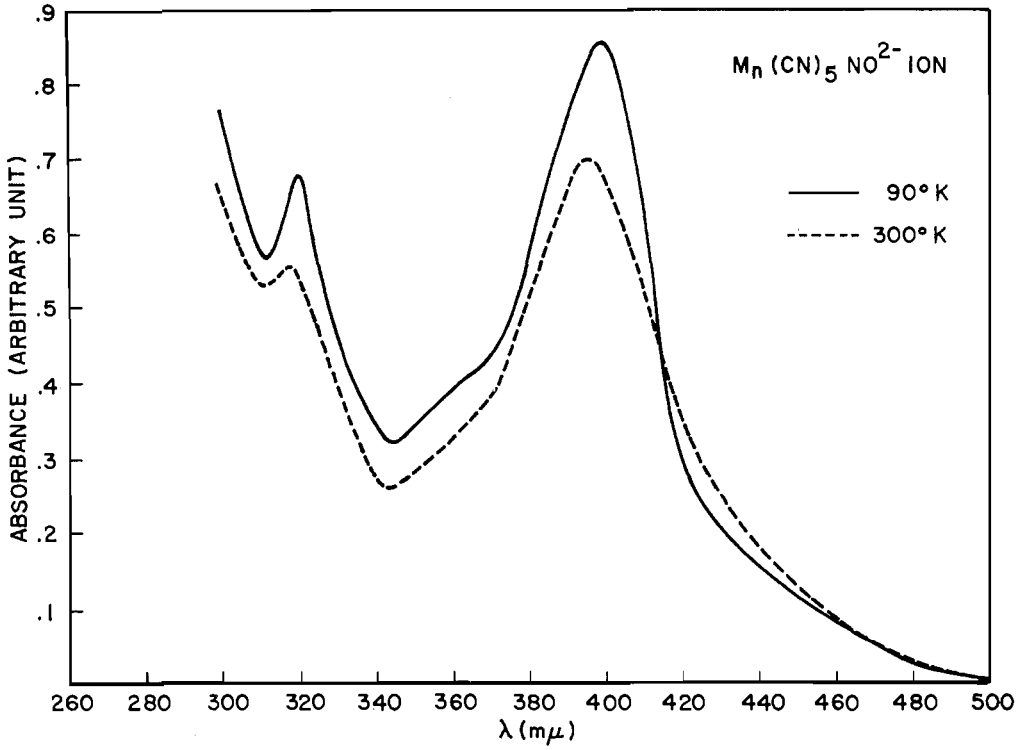

Figure 9.—Electronic spectra of $[(n\text{-}C_4H_9)_4N]_2[Mn(CN)_5NO]$ in EPA solution: dashed curve at 300°K; solid curve at 90°K.

ing an electron from the 6e to the 7e level, the energy required for the transition $^2B_2 \rightarrow {}^2B_2(6e \rightarrow 7e)$ is much less than the sum of the energies of the transitions $^2B_2 \rightarrow {}^2E(6e \rightarrow 2b_2)$ and $^2B_2 \rightarrow {}^2E(2b_2 \rightarrow 7e)$. It is consistent that the calculated one-electron energies for the 6e → 7e transition of 26,550 and 26,170 cm^{-1} for $Cr(CN)_5NO^{3-}$ and $Mn(CN)_5NO^{2-}$, respectively, are higher than the observed energies of 22,200 and 25,960 cm^{-1}.

Further remarks about the 22,200 cm^{-1} band in $Cr(CN)_5NO^{3-}$ are of interest here, since all the CrL_5NO^n complexes examined to date have a characteristic band at approximately 22,000 cm^{-1}. It is remarkable that the ions $Cr(CN)_5NO^{3-}$, $Cr(H_2O)_5NO^{2+}$, $Cr(C_2H_5OH)_5NO^{2+}$, and $Cr(NH_3)_5NO^{2+}$ have similar bands at 22,200 (ϵ 72), 22,370 (ϵ 131), 21,800 (ϵ 61), and 21,880 cm^{-1} (ϵ 69),[26,27] respectively. Since the M≡NO structure is present in all cases, the conclusion appears inescapable that the transition responsible for this band must be localized in the M≡NO unit. Again we have evidence of strong π bonding between the metal and the nitric oxide, usually considered formally as M→NO π bonding. Since the levels 6e and 7e give the degree of M→NOπ bonding, their observed nearly constant separation indicates that the degree of Cr→NO π bonding is substantially the same in all these complexes. Also consistent with this assertion is the fact that the N–O stretching frequencies in these complexes have similar values. Thus we have 1645, 1670, 1747, 1719, and 1718 cm^{-1}, respectively, for $Cr(CN)_5NO^{3-}$, $Cr(NH_3)_5NO^{2+}$, $Cr(H_2O)_5NO^{2+}$, $Cr(CH_3OH)_5NO^{2+}$, and $Cr(C_2H_5OH)_5NO^{2+}$.[26] These results again support our model in which the metal–nitric oxide bonding dominates the over-all ligand field.

The low-temperature spectra of $Cr(CN)_5NO^{3-}$ and $Mn(CN)_5NO^{2-}$ are shown in Figures 8 and 9. The $Mn(CN)_5NO^{2-}$ spectrum at low temperature shows a sharpening of the 25,960 cm^{-1} band, and the $Cr(CN)_5NO^{3-}$ band at 22,200 cm^{-1} shows vibrational fine structure. The intensities of both the bands are not changed substantially at the low temperature, indicating that they are of allowed electronic origin, in agreement with our assignment $^2B_2 \rightarrow {}^2B_2(6e \rightarrow 7e)$. The spectrum of $Cr(CN)_5NO^{3-}$ at the low temperature shows a vibrational progression on the low-energy side of the 22,220 cm^{-1} band. The energy separations decrease as the spectrum moves to the higher energy side. The peak separations of 566, 507, 468, 468, 465, and 362 cm^{-1} can be explained in terms of a vibronic progression. The Cr–N stretching frequency is 618.5 cm^{-1} in the ground electronic state. The transfer of an electron from the 6e to the 7e level should weaken the Cr–N bond and thereby decrease the stretching frequency, as is observed. The separations 566, 507, 468, 468, and 465 cm^{-1} appear as the Cr–N vibronic progression involving the populated vibrational levels of the ground electronic state and appropriate vibrational levels of the excited electronic state. The separation 362 cm^{-1} may represent the excited state Cr–C stretching frequency, which should also be lower than the ground-state stretching frequency of 400 cm^{-1}. This is reasonable because the 7e level has some π^*CN character.

Similar vibrational fine structure was observed in the low-temperature spectrum of the complex $Cr(NH_3)_5NO^{2+}$. The vibronic bands are found on the low-energy side of the 21,880 cm^{-1} maximum and the

(26) W. P. Griffith, *J. Chem. Soc.*, 3286 (1963).
(27) E. F. Hockings and I. Bernal, *ibid.*, 5029 (1964).

energy separations are 536, 468, 513, 490, 486, 435, and 477 cm^{-1}.[28] It is probable that a low-temperature study of $Cr(H_2O)_5NO^{2+}$ and $Cr(C_2H_5OH)_5NO^{2+}$ would reveal the same kind of fine structure.

The shoulders at 27,320 cm^{-1} for $Cr(CN)_5NO^{3-}$ and 28,570 cm^{-1} for $Mn(CN)_5NO^{2-}$ are assigned to the orbitally-forbidden $^2B_2 \rightarrow {}^2B_1(2b_2 \rightarrow 3b_1)$ transition. In this transition a near zero interelectronic-repulsion change is expected in the *xy* plane.[6] The calculated one-electron energies of 28,260 cm^{-1} for $Cr(CN)_5NO^{3-}$ and 32,530 cm^{-1} for $Mn(CN)_5NO^{2-}$ are in reasonably good agreement with the observed spectral values. Additional support for the $^2B_2 \rightarrow {}^2B_1$ band assignments comes from the low-temperature spectra. In $Cr(CN)_5NO^{3-}$, the 27,320 cm^{-1} band has reduced intensity at the low temperature, confirming the orbitally-forbidden nature of the band. Unfortunately, in $Mn(CN)_5NO^{2-}$ the shoulder is not resolved well and it is difficult to assess its exact intensity at either room or low temperature.

The absorption bands with maxima at 37,300 and 32,280 cm^{-1} for $Cr(CN)_5NO^{3-}$ and $Mn(CN)_5NO^{2-}$, respectively, are assigned as the ligand-to-metal type charge-transfer transition $^2B_2 \rightarrow {}^2E(5e \rightarrow 2b_2)$. For low-spin complexes in which the metal furnishes fewer than six valence electrons (such as the d^5 $Fe(CN)_6^{3-}$), additional charge-transfer bands due to ligand-to-metal transitions are expected at low energies.[29] Naiman[29a,29c] assigned the band at 24,100 cm^{-1} in $Fe(CN)_6^{3-}$ as ligand-to-metal type charge transfer and the general assignment has been accepted by Basu and Belford,[29b] even though there has been some dispute[29] as to the exact transition responsible for this band. We also note that ligand-to-metal type charge transfer in an analogous series of complexes shifts to lower energy on increasing the positive charge on the central metal ion. This is demonstrated nicely in the $PtCl_4^{2-}$ and $AuCl_4^-$ complexes.[24] Therefore, we conclude that the bands at 37,300 cm^{-1} in $Cr(CN)_5NO^{3-}$ and 32,280 cm^{-1} in $Mn(CN)_5NO^{2-}$ represent ligand-to-metal charge-transfer transitions. Comparing "d^5" systems $Fe(CN)_6^{3-}$, $Mn(CN)_5NO^{2-}$, and $Cr(CN)_5NO^{3-}$, the formal charge on the central metal ion decreases in the order Fe(III) > Mn(II) > Cr(I). As the positive charge on the central metal decreases, there is an increase in the transition energy, namely 24,100 < 32,280 < 37,300 cm^{-1}. It is is noteworthy that the ligand-to-metal transition in $Fe(CN)_6^{3-}$ is from a ligand π-type level (π_{CN}) to the t_{2g} level. Similarly, the $^2B_2 \rightarrow {}^2E$ ($5e \rightarrow 2b_2$) transitions in $Mn(CN)_5NO^{2-}$ and $Cr(CN)_5NO^{3-}$ are from an almost pure ligand π_{CN} level to a metal d_π-type level. Further support for the assignment of the 32,280 cm^{-1} band in $Mn(CN)_5NO^{2-}$ as an orbitally-allowed transition is derived from the low-temperature spectra. The intensity of this band slightly increases at the low temperature. The calculated values of 37,420 and 28,830 cm^{-1} for these transitions in $Cr(CN)_5NO^{3-}$ and $Mn(CN)_5NO^{2-}$ are in moderately good agreement with the observed values of 37,300 and 32,280 cm^{-1}.

The 43,480 cm^{-1} band in $Cr(CN)_5NO^{3-}$ and the 48,540 cm^{-1} band in $Mn(CN)_5NO^{2-}$ are assigned as metal-to-π^*CN charge-transfer bands, specifically $^2B_2 \rightarrow {}^2E(2b_2 \rightarrow 8e)$. In the diamagnetic $Mn(CN)_5NO^{3-}$ complex, the transition $^1A_1 \rightarrow {}^1E_2(2b_2 \rightarrow 8e)$ occurs at 45,450 cm^{-1}. The higher position of the $2b_2 \rightarrow 8e$ band in $Mn(CN)_5NO^{2-}$ is partly due to the higher positive charge on Mn in $Mn(CN)_5NO^{2-}$ than in $Mn(CN)_5NO^{3-}$. Since the stability of the "metal" level $2b_2$ should increase in the order Cr(I) < Mn(II), we expect the transition $^2B_2 \rightarrow {}^2E(2b_2 \rightarrow 8e)$ to occur at a lower energy in $Cr(CN)_5NO^{3-}$ than in $Mn(CN)_5NO^{2-}$. Thus the values of 43,480 cm^{-1} for $Cr(CN)_5NO^{3-}$ and 48,540 cm^{-1} for $Mn(CN)_5NO^{2-}$ at the very least are internally consistent. However, the calculated one-electron energy separations of 35,680 and 45,050 cm^{-1}, respectively, for $Cr(CN)_5NO^{3-}$ and $Mn(CN)_5NO^{2-}$, are very much lower than the observed values. Recall that the predicted energies for the same transition in $V(CN)_5NO^{5-}$ and $Mn(CN)_5NO^{3-}$ are lower than the spectroscopic values. A possible reason for the low calculated energy for this transition has been discussed earlier in the section on the assignments of spectral bands in $V(CN)_5NO^{5-}$.

There is only one band in $Mn(CN)_5NO^{2-}$ left to be assigned. The band appears at 37,030 cm^{-1}, and we suggest that it be assigned as the orbitally-allowed transition $^2B_2 \rightarrow {}^2E(6e \rightarrow 5a_1)$. The same transition in the diamagnetic $Mn(CN)_5NO^{3-}$ occurs at 37,850 cm^{-1}. Moreover, the calculated energy separation (corrected for interelectronic repulsion) of 38,740 cm^{-1} is in good agreement with the spectral value.

Molecular Orbitals and the Esr Results.—The various spin Hamiltonian parameters have been used to calculate molecular orbital parameters and to establish the electronic structures of several metal complexes.[8,30-33] As a further test of our molecular orbitals in $M(CN)_5NO^{n-}$ complexes, we shall attempt to calculate the spin Hamiltonian parameters in the paramagnetic systems which have been extensively investigated using esr methods.

The complexes that will be considered here are $Cr(CN)_5NO^{3-}$ and $Mn(CN)_5NO^{2-}$. In the calculation, we shall consider only the excited states that are less than 60,000 cm^{-1} above the ground state. To make the calculations of the one-electron molecular orbitals tractable, we shall consider only those valence orbitals which are expected to contribute substantially to the values of the various A tensors and the g tensor. For example, we reject in the 6e and 7e levels the very small contributions of the p_x, p_y, σCN, π_hCN (equatorial), and π_h^*CN (equatorial) levels. Also in the π levels of NO, only the p orbitals of nitrogen will be considered because nitric oxide is bonded to the metal

(28) We measured this spectrum at the request of Professor I. Bernal.

(29) (a) C. S. Naiman, *J. Chem. Phys.*, **35**, 323 (1961); (b) G. Basu and R. L. Belford, *ibid.*, **37**, 1933 (1962); (c) C. S. Naiman, *ibid.*, **39**, 1900 (1963).

(30) A. H. Maki and B. R. McGarvey, *ibid.*, **29**, 31, 35(1958).

(31) W. Marshall and R. Stuart, *Phys. Rev.*, **123**, 2048 (1961).

(32) D. Kivelson and R. Neiman, *J. Chem. Phys.*, **35**, 149 (1961).

(33) D. Kivelson and S.-K. Lee, *ibid.*, **41**, 1896 (1964).

through nitrogen. Similarly, in the π levels of CN, we shall consider only the p orbitals of carbon. On the basis of these approximations, the relevant molecular orbitals are given as follows.[34]

$$\Psi(1b_1) = \beta_1 d_{x^2-y^2} + \frac{\beta_1'}{2}(\sigma_1 - \sigma_2 + \sigma_3 - \sigma_4) \quad (12)$$

$$\Psi(3b_1) = \beta_1^* d_{x^2-y^2} - \frac{\beta_1'^*}{2}(\sigma_1 - \sigma_2 + \sigma_3 - \sigma_4) \quad (13)$$

$$\Psi(2b_2) = \beta_2^* d_{xy} - \frac{\beta_2'^*}{2}(\pi_{1h} - \pi_{2h} + \pi_{3h} - \pi_{4h}) \quad (14)$$

$$\Psi(6e) = \epsilon_{\pi 1} d_{xz} + \epsilon_{\pi 2}\pi_{5x} + \epsilon_{\pi 3}\pi_{6x} + \frac{\epsilon_{\pi 4}}{\sqrt{2}}(\pi_{1v} - \pi_{3v}) \quad (15)$$

$$\Psi(7e) = \epsilon_{\pi 1}^* d_{xz} - \epsilon_{\pi 2}^*\pi_{5x} - \epsilon_{\pi 3}\pi_{6x} - \frac{\epsilon_{\pi 4}^*}{\sqrt{2}}(\pi_{1v} - \pi_{3v}) \quad (16)$$

The σ orbital of carbon in σCN is defined as $\sigma_k = n(2p)_k + (1 - n^2)^{1/2}(2s)_k$. All the coefficients have been determined in the molecular orbital calculations.

The appropriate spin Hamiltonian $\mathcal{H}$ for $M(CN)_5NO^{n-}$ is given by

$$\mathcal{H} = \beta[g_{||}S_zH_z + g_\perp(S_xH_x + S_yH_y)] + [(A^M)S_zI_z^M + B^M(S_xI_x^M + S_yI_y^M)] \quad (17)$$

In eq 17 $(z,||)$ and $(x,y,\perp)$ refer to the directions parallel and perpendicular to the NC–M–NO bond.

The g factor for a paramagnetic molecule with an orbitally nondegenerate ground state differs from 2.0023 due to the mixing of the ground state and the excited states *via* spin-orbital coupling. Following the treatment of Maki and McGarvey,[30] Kivelson and Neiman,[32] and Kivelson and Lee[33] and using the functions (12)–(16) we have obtained expressions for the various spin Hamiltonian parameters in terms of the molecular orbital coefficients, spin-orbital coupling constants, electronic transition energies, and values of appropriate overlap integrals.

g Values.—We consider the excitations $1b_1 \rightarrow 2b_2$ and $2b_2 \rightarrow 3b_1$ as the most important contributors to the $g_{||}$ value and the excitations $6e \rightarrow 2b_2$ and $2b_2 \rightarrow 7e$ as the most important contributors to $g_\perp$. These excited states contaminate the ground state *via* spin-orbital coupling. Using the molecular orbitals (12)–(16), we arrived at the following expressions for $g_{||}$ and $g_\perp$.

$$g_{||} = 2.0023 - \frac{8|\lambda|(\beta_1^*)^2(\beta_2^*)^2}{\Delta E(3b_1 - 2b_2)} \times \left[1 - \frac{1}{2}\left(\frac{\beta_1'^*\beta_2'^*}{\beta_1^*\beta_2^*}\right)T(n) - \left(\frac{\beta_1'^*}{\beta_1^*}\right)S - \left(\frac{\beta_2'^*}{\beta_2^*}\right)\pi\right] + \frac{8|\lambda|(\beta_1)^2(\beta_2^*)^2}{\Delta E(2b_2 - 1b_1)}\left[1 + \frac{1}{2}\left(\frac{\beta_1'\beta_2'^*}{\beta_1\beta_2^*}\right)T(n) + \left(\frac{\beta_1'}{\beta_1}\right)S - \left(\frac{\beta_2'^*}{\beta_2^*}\right)\pi\right] \quad (18)$$

$$g_\perp = 2.0023 - \frac{2|\lambda|(\beta_2^*)^2(\epsilon_{\pi 1}^*)^2}{\Delta E(7e - 2b_2)}\left[1 - \left(\frac{\beta_2'^*}{\beta_2^*}\right)\pi - \left(\frac{\epsilon_\pi^*{}_2}{\epsilon_{\pi 1}^*}\right)\pi_1 - \left(\frac{\epsilon_{\pi 3}^*}{\epsilon_{\pi 1}^*}\right)\pi_2 - \sqrt{2}\left(\frac{\epsilon_{\pi 4}^*}{\epsilon_{\pi 1}^*}\right)\pi_2 + \left(\frac{\epsilon_{\pi 4}^*\beta_2'^*}{\epsilon_{\pi 1}^*\beta_2^*}\right)\left(\frac{1}{\sqrt{2}}\right)\right] + \frac{2|\lambda|(\beta_2^*)^2(\epsilon_{\pi 1})^2}{\Delta E(2b_2 - 6e)}\left[1 - \left(\frac{\beta_2'^*}{\beta_3^*}\right)\pi + \left(\frac{\epsilon_{\pi 2}}{\epsilon_{\pi 1}}\right)\pi_1 + \sqrt{2}\left(\frac{\epsilon_{\pi 4}}{\epsilon_{\pi 1}}\right)\pi_2 + \left(\frac{\epsilon_{\pi 3}}{\epsilon_{\pi 1}}\right)\pi_2 - \left(\frac{\epsilon_{\pi 4}\beta_2'^*}{\epsilon_{\pi 1}\beta_2^*}\right)\left(\frac{1}{\sqrt{2}}\right)\right] \quad (19)$$

Here $|\lambda|$ is the spin-orbital coupling constant for the complex referred to the central metal ion and $T(n)$ is defined by

$$T(n) = n + \frac{(1 - n^2)^{1/2}}{\sqrt{3}} R \int_0^\infty r^2 R_{21}(r)\frac{d}{dr}[R_{20}(r)]\,dr \quad (20)$$

A simple method of evaluating $T(n)$ has been given.[30] Overlap integrals are defined as follows.

$$S = 2\langle d_{x^2-y^2}|\sigma CN\rangle \quad (21)$$

$$\pi = 2\langle d_{xy}|\pi CN\rangle \quad (22)$$

$$\pi_1 = \langle d_{xz}|\pi NO\rangle \quad (23)$$

$$\pi_2 = \langle d_{xz}|\pi CN\rangle \quad (24)$$

All the terms given in the brackets of (18) and (19) are derived from the calculation of matrix elements of the form[30]

$$\Lambda_{ij} = -2\sum_{n\neq 0}\frac{\langle B_2|\lambda(r)1_i|n\rangle\langle n|1_j|B_2\rangle}{E_n - E_0} \quad (25)$$

where the subscripts i and j refer to the cartesian coordinates x, y, and z, and n represents the various excited states B_1, E, etc. It should be mentioned that in the evaluation of eq 18 and 19, all integrations over the ligand orbitals that involve an inverse dependence on r were neglected.[30] It should also be noticed that in the integral $\langle n|1_j|B_2\rangle$ the approximation of neglecting the integration over the ligand orbitals has not been made. It is this expression which leads to the overlap integrals given above.

Using eq 18–24, the theoretical values for $g_{||}$ and $g_\perp$ were calculated for both complexes $Cr(CN)_5NO^{3-}$ and $Mn(CN)_5NO^{2-}$. It is necessary in these calculations to have a value for the spin-orbital coupling constant $|\lambda|$ for the chromium and the manganese ions in these complexes. The calculated charge distributions associated with chromium and manganese are $Cr^{+0.38}$ $[(3d)^{4.98}(4s)^{0.38}(4p)^{0.26}]$ and $Mn^{+0.36}$ $[(3d)^{5.92}(4s)^{0.43}(4p)^{0.28}]$. Thus we have taken $|\lambda| = 190$ cm^{-1} for Cr^+ $(3d^5)$ and $|\lambda| = 255$ cm^{-1} for $Mn^+(3d^6)$.[35]

Two different calculations were performed. In calculation I, all the parameters (except $|\lambda|$) in (18) and (19) are derived from the MO calculations. This includes transition energies. In calculation II, the same

(34) σ refers to the equatorial carbon part of a σCN orbital; π_h and π_v refer to the equatorial carbon p orbitals of πCN and π^*CN; π_{5x} refers to the nitrogen orbitals of πNO and π^*NO; π_{6x} refers to the axial carbon p orbitals of πCN and π^*CN.

(35) T. M. Dunn, *Trans. Faraday Soc.*, **57**, 1441 (1961).

TABLE IX

PARAMETERS USED FOR THE CALCULATION OF $g_{||}$, $g_{\perp}$, A, AND B VALUES

	$Cr(CN)_5NO^{3-}$		$Mn(CN)_5NO^{2-}$	
	Calcn I	Calcn II	Calcn I	Calcn II
λ	190 cm^{-1}		255 cm^{-1}	
ΔE ($3b_1 \rightarrow 2b_2$)	28,260	27,320	32,530	28,570
ΔE ($2b_2 \rightarrow 1b_1$)	58,000[a]	58,000[a]	50,000[a]	50,000[a]
ΔE ($7e \rightarrow 2b_2$)	13,890	15,380	18,340	18,600
ΔE ($2b_2 \rightarrow 6e$)	12,660	13,700	7,820	12,050
$T(n)$	0.7956[b]		0.7956[b]	
S	0.273		0.260	
π	0.2412		0.2068	
π_1	0.1261		0.1113	
π_2	0.1161		0.1017	
β_1	0.4486		0.6362	
β_1'	0.6670		0.6236	
β_1^*	0.8593		0.8171	
$\beta_1'^*$	0.7973		0.8171	
β_2^*	0.9121		0.9293	
$\beta_2'^*$	0.1795		0.3314	
$\epsilon_{\pi 1}$	0.5992		0.7233	
$\epsilon_{\pi 2}$	0.9325		0.6396	
$\epsilon_{\pi 3}$	−0.118		−0.1547	
$\epsilon_{\pi 4}$	−0.2449		−0.2847	
$\epsilon_{\pi 1}^*$	0.7129		0.6075	
$\epsilon_{\pi 2}^*$	1.4111		1.5694	
$\epsilon_{\pi 3}^*$	−0.1044		0.0341	
$\epsilon_{\pi 4}^*$	0.1015		0.0415	

[a] An estimated interelectronic-repulsion energy of 10,000 cm^{-1} was added to the calculated one-electron separation. [b] To simplify the calculation, the value of n in the expression for $T(n)$ was taken from the CN function, but the effective nuclear charges were estimated using Hartree's formula [D. R. Hartree, "The Calculation of Atomic Structures," John Wiley and Sons, Inc., New York, N. Y., 1957, pp 117, 167].

$|\lambda|$ values and molecular orbital coefficients are used with the observed transition energies. Table IX gives the parameter values used in the two calculations. Table X gives the calculated and experimental values of $g_{||}$ and $g_{\perp}$.

It is gratifying that the g values, calculated by using the molecular orbital coefficients and the theoretical transition energies, are very close to the experimental values. Our neglect of the low-energy transition $5e \rightarrow 2b_2$ can be cited as the cause of the calculated $g_{\perp}$ values being slightly lower than the observed values. Since the contribution from the $5e \rightarrow 2b_2$ transition will be positive, the calculated $g_{\perp}$ values would increase. Calculation II, with the observed transition energies instead of the calculated energies, is not substantially different from calculation I. We conclude that the calculated molecular orbitals and the electronic spectral assignments are consistent with the observed g values in $Cr(CN)_5NO^{3-}$ and $Mn(CN)_5NO^{2-}$.

Metal Hyperfine Interactions.—Using the same kind of approximations employed to calculate $g_{||}$ and $g_{\perp}$, we have derived the following theoretical expressions for the metal splitting constants

$$A^M = P_M\left[-(\beta_2^*)^2\left(\frac{4}{7}+\kappa_M\right) - \frac{8|\lambda|(\beta_1^*)^2(\beta_2^*)^2}{\Delta E(3b_1 - 2b_2)} + \frac{8|\lambda|(\beta_1)^2(\beta_2^*)^2}{\Delta E(2b_2 - 1b_1)} - \frac{\frac{6}{7}|\lambda|(\beta_2^*)^2(\epsilon_{\pi 1}^*)^2}{\Delta E(7e - 2b_2)} + \frac{\frac{6}{7}|\lambda|(\beta_2^*)^2(\epsilon_{\pi 1})^2}{\Delta E(2b_2 - 6e)}\right] \quad (26)$$

$$B^M = P_M\left[(\beta_2^*)^2\left(\frac{2}{7}-\kappa_M\right) - \frac{\frac{11}{7}|\lambda|(\beta_2^*)^2(\epsilon_{\pi 1}^*)^2}{\Delta E(7e - 2b_2)} + \frac{\frac{11}{7}|\lambda|(\beta_2^*)^2(\epsilon_{\pi 1})^2}{\Delta E(2b_2 - 6e)}\right] \quad (27)$$

where P_M is given as[36]

$$P_M = 2\gamma_M\beta\beta_n\langle 3d|r_M^{-3}|3d\rangle \quad (28)$$

γ_M is the gyromagnetic ratio of the metal, β_n is the nuclear magneton, r_M is the distance from the nucleus of M to the unpaired electron, and κ_M is the Fermi contact interaction term, given by the equation[36]

$$\kappa_M = -\left(\frac{32\pi\gamma_M\beta\beta n}{3P_M}\right)\langle 0|\sum_k \delta(r_{Mk})S_{zk}|0\rangle \quad (29)$$

where 0 refers to the ground state, r_{Mk} is the displacement from the Mth nucleus to the kth electron, s_{zk} is the spin operator for the kth electron, and δ the δ-function operator evaluated in the ground state.

TABLE X

CALCULATED AND MEASURED SPIN HAMILTONIAN PARAMETERS

	$Cr(CN)_5NO^{3-}$			$Mn(CN)_5NO^{2-}$		
	Calcn I	Calcn II	Exptl	Calcn I	Calcn II	Exptl
$g_{||}$	1.9882	1.9874	1.9722	2.0020	1.9994	1.9922
$g_{\perp}$	2.0040	2.0040	2.0044	2.0273	2.0167	2.0311
$g_{\perp}/g_{||}$	1.0080	1.0084	1.0163	1.0126	1.0086	1.0195
$\lvert A - B\rvert$, cm^{-1}		2.0505×10^{-3}	2.0085×10^{-3}		12.285×10^{-3}	11.526×10^{-3}
κ		0.7600			0.4833	

Equations 26 and 27 can be rewritten with the help of eq 18 and 19, as follows

$$A^M = P_M\left[-(\beta_2^*)^2\left(\frac{4}{7}+\kappa_M\right) + (g_{||} - 2.0023) + \frac{3}{7}(g_{\perp} - 2.0023) + D_{||} + \frac{3}{7}D_{\perp}\right] \quad (30)$$

$$B^M = P_M\left[(\beta_2^*)^2\left(\frac{2}{7}-\kappa_M\right) + \frac{11}{14}(g_{\perp} - 2.0023) + \frac{11}{14}D_{\perp}\right] \quad (31)$$

(36) A. Abragam, J. Horowitz, and M. H. L. Pryce, *Proc. Roy. Soc.* (London), **A230**, 169 (1955).

where $D_{\|}$ and $D_{\perp}$ are small corrections which can be calculated from (18) and (19). The calculated $D_{\|}$ and $D_{\perp}$ values are -0.01486 and -0.0039 for $Cr(CN)_5NO^{3-}$ and -0.0241 and -0.0040 for $Mn(CN)_5NO^{2-}$. Using the observed g values and derived MO coefficients, values have been calculated for $|A - B|$. The results are given in Table X. We have used the value of Kuska and Rogers[8] for P_{Cr}. A value for P_{Mn} has been calculated using $\langle r^{-3} \rangle = 5.38$ au[37] and $\gamma_{Mn} = 1.387$.[36] The calculated and observed $|A - B|$ values are in very close agreement, indicating again that the derived molecular orbitals are quite satisfactory.

The Fermi contact interaction constants κ_{Cr} and κ_{Mn} have been estimated. The values are listed in Table X. They were calculated using (30) and (31), with the experimental $g_{\|}$, $g_{\perp}$, A, and B values and the calculated P_M values. The κ_{Mn} value of 0.4833 is in close agreement with the value obtained for Mn^{2+} ion by Abragam, *et al.*[36] The nonvanishing value for κ_M suggests that the unpaired electron has metal s character. A nonvanishing value of κ_M can be obtained by including configurations obtained by exciting an electron from a filled orbital with s character to an unfilled one with s character and of the same symmetry.[36] We know from the orbital transformation scheme that the metal 4s transforms as the a_1 representation. So the Fermi contact interaction can be explained by considering the excitation of an electron from one of the filled a_1 levels to one of the unfilled levels with a_1 symmetry. We have not carried out a detailed analysis.

The very large values for β_2^*, namely 0.9121 for $Cr(CN)_5NO^{3-}$ and 0.9293 for $Mn(CN)_5NO^{2-}$ (from the MO calculations) indicate that the $2b_2$ electron is essentially localized on the metal d_{xy} orbital. The fact that the calculated and measured $|A - B|$ values are in good agreement supports this interpretation.

Extrahyperfine Structure.—The isotropic extrahyperfine splittings due to the ^{14}N of NO are 5.70 and 3.80 gauss for $Cr(NO)_5NO^{3-}$ and $Mn(CN)_5NO^{2-}$, respectively. This suggests that the unpaired electron in each case has nitrogen s character. The σNO orbital, which includes a contribution from 2s(N), transforms as the a_1 representation. In a configuration-interaction treatment[36] the excited configurations of interest are those obtained by promoting an electron from a field a_1 orbital with nitrogen s character to an unoccupied a_1 level. For both $Cr(CN)_5NO^{3-}$ and $Mn(CN)_5NO^{2-}$, the extrahyperfine tensors due to ^{14}N have been found to be anisotropic. The values are given in Table I. Since the $2b_2$ molecular orbital does not include any contribution from NO orbitals, the anisotropic splitting constants present a problem. Possible mechanisms to place spin density on π^*NO in the ground state have been discussed by Fortman and Hayes.[38] An attractive possibility is the scrambling of configurations $^2B_2(6e^4 2b_2^1)$ and $^2B_2(6e^3 2b_2^1 7e^1)$ *via* a nonvanishing matrix element of interelectronic repulsion. According to the present electronic spectral analysis, these two $^2B_2$ states are separated by *ca.* 25,000 cm^{-1} in the complexes. The fact that the A^N and B^N values for $Cr(CN)_5NO^{3-}$ are larger than for $Mn(CN)_5NO^{2-}$ is consistent with the calculated molecular orbitals of these complexes, since the product $(e_{\pi 2})^2(e_{\pi 2}^*)^2$ is larger for $Cr(CN)_5NO^{3-}$ by a factor of 1.62. For comparison, the ratios $A^N(Cr):A^N(Mn)$ and $B^N(Cr):B^N(Mn)$ are 1.52 and 1.49, respectively.

The extrahyperfine constants due to ^{13}C in $Cr(CN)_5NO^{3-}$ have been measured accurately.[8,38] The equatorial ^{13}C splitting provides important information on the degree of delocalization in the $2b_2$ orbital. Fortman and Hayes have obtained[38] a value of 0.173 for the molecular orbital coefficient $\beta_2'^*$ from the measured anisotropic ^{13}C extrahyperfine constants. For comparison, we have obtained $\beta_2'^* = 0.1795$ from the molecular orbital calculation. Thus the analysis of the anisotropic splitting constants due to ^{53}Cr and $^{13}C_{eq}$ in $Cr(CN)_5NO^{3-}$ and ^{55}Mn in $Mn(CN)_5NO^{2-}$ gives $2b_2$ molecular orbitals which are essentially the same as those obtained from the SCCC–MO calculations. The fact that the calculated molecular orbitals are consistent with *both* the electronic spectral and magnetic data is extremely encouraging.

Acknowledgments.—We thank Mr. J. Pearlman for help with some of the infrared spectral measurements and Mr. J. Halper and Mr. J. Preer for checking a number of calculations. This research was supported by the National Science Foundation.

(37) V. S. Krol'kov, *Opt. Spectry.*, **11**, 73 (1961).

(38) J. J. Fortman and R. G. Hayes, *J. Chem. Phys.*, **43**, 15 (1965).